Reliable and Efficient Sparse Code Spreading Aided MC-DCSK Transceiver Design for Multiuser Transmissions

Zuwei Chen[®], Lin Zhang[®], Senior Member, IEEE, Zhiqiang Wu[®], Senior Member, IEEE, Lin Wang[®], Senior Member, IEEE, and Weikai Xu[®], Member, IEEE

Abstract-In this paper, we propose a Sparse Code Spreading-aided Multi-Carrier Differential Chaos Shift Keying (SCS-MC-DCSK) transceiver to improve the efficiency and reliability performances for multiuser transmissions. With the aim to improve the spectrum efficiency and enhance the reliability, we construct a multi-dimension codebook based on a factor graph matrix to spread information bits in a non orthogonal way, thus the signals could overlap and multiple users are allowed to share all sub-carrier resources via the non orthogonal spreading. The information bits using the same codebook are regarded as a layer, while each user could choose to use one or multiple layers. Then the resultant symbols are spread by the reference chaotic sequence and its quadrature version generated by Hilbert transform in the time domain. At the receiver, reverse operations are conducted, and we propose the Minimum Distance (MD) detection method to retrieve the estimates. Furthermore, theoretical performances, including the Symbol Error Rate (SER), capacity, energy efficiency, spectrum efficiency and computational complexity, are analyzed and compared among the proposed design and benchmarks. Simulation results are then provided to validate the theoretical analysis. Moreover, the Bit Error Rate (BER) performances under different channel conditions demonstrate the superior reliability and efficiency to benchmarks.

Manuscript received May 16, 2020; revised September 23, 2020; accepted November 17, 2020. Date of publication November 25, 2020; date of current version March 17, 2021. This work was supported Guangdong Basic and Applied Basic Research Foundation (No. 2020A1515010703), the Key Research and Development and Transformation Plan of Science and Technology Program for Tibet Autonomous Region (No. XZ201901-GB-16), the Project of National Natural Science Foundation of China (No. 61671395, No. 61602531, and No. 61871337), and in part supported by Guangdong Science and Technology Project (No. 2020A1010020009). The associate editor coordinating the review of this article and approving it for publication was L. Wei. (Corresponding author: Lin Zhang.)

Zuwei Chen is with the School of Electronics and Information Technology, Sun Yat-sen University, Guangzhou 510006, China (e-mail: chenzw25@mail2.sysu.edu.cn).

Lin Zhang is with the School of Electronics and Information Technology, Sun Yat-sen University, Guangzhou 510006, China, and also with the Southern Marine Science and Engineering Guangdong Laboratory, Zhuhai 519000, China (e-mail: isszl@mail.sysu.edu.cn).

Zhiqiang Wu is with the Department of Electrical Engineering, Tibet University, Lhasa 850000, China, and also with the Department of Electrical Engineering, Wright State University, Dayton, OH 45435 USA (e-mail: zhiqiang.wu@wright.edu).

Lin Wang and Weikai Xu are with the Department of Electrical Engineering, Xiamen University, Xiamen 361005, China (e-mail: wanglin@xmu.edu.cn; xweikai@xmu.edu.cn).

Color versions of one or more figures in this article are available at https://doi.org/10.1109/TCOMM.2020.3040422.

Digital Object Identifier 10.1109/TCOMM.2020.3040422

Index Terms—Minimum distance detection, multi carrier differential chaos shift keying, non orthogonal sparse code spreading, spectrum efficiency, symbol error rate (SER).

I. Introduction

HAOTIC signals have a wide range of potential applications in wireless systems to enhance the physical layer security and resist the jamming [1], [2] or the interferences, thanks to their natural properties such as being aperiodic and sensitive to the initial value [3].

Since the non-coherent chaotic modulation scheme, Differential Chaos Shift Keying (DCSK) [4], removes the complex chaotic synchronization circuit required by the coherent chaotic modulation, they have attracted more research interests than coherent chaotic modulation schemes. Moreover, the applications of the DCSK scheme in wireless systems including cooperative communication systems [5], relay communication systems [6], mobile communication systems [7], Ultra Wide Band (UWB) systems [8] as well as Simultaneous Wireless Information and Power Transfer (SWIPT) systems [9] have been well investigated.

However, in DCSK systems, half the bit duration is required for the delivery of reference chaotic signals, while the delay lines used for the differential operation is difficult for implementations. Many research works have put efforts to improve the data rate and the practicality of DCSK transceivers.

A. Related Research Works

Researchers have utilized resources in the time, code, space and the frequency domains to address the above issues. For example, the Quadrature Chaos Shift Keying (QCSK) scheme [10] adopts Hilbert transform to construct a quadrature chaotic signal to deliver more bits, while in [11], a Spatial Modulation (SM) (SM-DCSK) scheme utilizes the space domain to improve the efficiency. In addition, [12] has proposed a Pulse Position Modulation (PPM) scheme to exploit the position of pulses to modulate more bits while [13] extends PPM-DCSK scheme to the Multi-User (MU) scenarios with low complexity, high energy efficiency and data rate. Moreover, to remove the delay lines, a Code-Shifted DCSK (CS-DCSK) [14] scheme is presented to separate the reference and the data by Walsh codes. Furthermore, higher

0090-6778 © 2020 IEEE. Personal use is permitted, but republication/redistribution requires IEEE permission. See https://www.ieee.org/publications/rights/index.html for more information.

order modulation schemes are proposed, such as the Multilevel CS-DCSK (MCS-DCSK) [15] method which uses high order Walsh code, and the MCS-DCSK with *M*-ary Modulation (MCS-MDCSK) [16] as well as the MCS-DCSK with Code Index Modulation (CIM-MCS-DCSK) [17] schemes to improve the data rate. Except for these achievements on enhanced efficiency performances, research works have also been done to improve the reliability performances. For example, a Frequency Modulation (FM) scheme is proposed to keep the symbol energy constant [18], then a low-complexity energy detector is presented for the FM-DCSK system to combat the narrow interferences [8].

In the frequency domain, the Multi-Carrier DCSK system (MC-DCSK) [19] has been proposed to utilize orthogonal multiple subcarriers to remove the delay line and to improve the efficiency via allowing multiple information bearing signals to share one reference signal. Then the improved versions of the MC-DCSK system are proposed [20]–[23] to improve performances including the energy efficiency, spectral efficiency and the reliability.

In order to further enhance MC-DCSK system performances, the carrier index is utilized in [20] to improve Bit Error Rate (BER) performances, spectral efficiency and energy efficiency. Then this scheme was further extended in [21] to flexibly adjust the number of both index carriers and index bits to enhance the practicality. Furthermore, in [22], the authors proposed a hierarchical-modulation scheme called Multi-Carrier M-ary DCSK system with Code Index Modulation (CIM-MC-M-DCSK) which applied the M-ary modulation for information-bearing signals over the cosinoidal carriers and the index modulation for the reference chaotic signal spread by Walsh codes over the sinusoidal carriers, to improve the BER performances and flexibly serve different quality of service demands. Furthermore, [9] proposed a new Multiple-Input-Single-Output (MISO) SWIPT scheme for CIM-MC-M-DCSK system [22] suitable for e-health internet of things applications. Moreover, in [23], the Gram-Schmidt algorithm is used to generate orthogonal chaotic basis to improve the data rate, energy efficiency and spectrum efficiency for MC-DCSK systems. Additionally, the authors proposed to perform carrier interference code to suppress the Peak-to-Average Power Ratio (PAPR) [24].

Additionally, the MC-DCSK schemes applies in MU scenarios are also investigated in [25]–[27]. Among these schemes, the orthogonal subcarriers are respectively used to deliver the information-bearing signals and the dedicated reference chaotic signals in [25], while in [26], only multiple reference chaotic signals are delivered separately over different subcarriers whereas the information-bearing signals can be overlapped and share the sub-bands. Then in [27], the analog network coding is applied to improve the spectrum efficiency and the energy efficiency.

In our previous works [28], [29], we proposed improved MC-DCSK schemes to respectively enhance the reliability or the robustness for the data respectively delivered via a specific subcarrier. In [28], we presented a general iterative receiver to improve the reliability performances with no need to change the MC-DCSK transmitter structure, while in [29],

we proposed to exploit the frequency diversity gain via the frequency hopping to enhance the robustness to channel condition variations over non contiguous bands.

To briefly sum up, most of the MC-DCSK and improved designs deliver the data via orthogonal codes or subcarriers. Although in [26] the chaotic modulated symbols can be overlapped, since chaotic sequences are non orthogonal, the transmissions would suffer from severe Multi-User Interferences (MUIs) which degrades the reliability performances.

B. Motivation and Contributions

Although a lot of research achievements have been presented to improve the performances of chaotic transmissions, few research works take account of the skyrocketing throughput demand and massive connectivity. When the number of User Equipments (UEs) is large, the performance degradations induced by the interferences between chaotic chips will become intolerable, and the spectrum efficiency is lowered by the delivery of multiple reference chaotic signals.

Our motivation is to improve the reliability and the data rate for chaotic systems serving a large number of UEs. In our design, inspired by the Sparse Code Multiple Access (SCMA) scheme [30]–[34] which utilizes the multi-dimensional codebook to achieve non-orthogonal spreading, we propose to exploit the sparse code spreading and multi-dimensional codebook to allow the overlapping of chaotic signals.

Different from the existing research works based on the orthogonal signal processing, in this paper, we propose a Sparse Code Spreading-aided Multi-Carrier Differential Chaos Shift Keying (SCS-MC-DCSK) transceiver, wherein the data sharing the same reference chaotic signal would overlap over subcarriers in an non-orthogonal way. Our objective is to improve the spectrum efficiency while retaining satisfactory reliability performances.

In the proposed SCS-MC-DCSK system, at the transmitter, we construct the sparse codebook, and the information bits from a specific user are mapped to a predefined sparse codeword. Thus a multi-dimension constellation modulation is implemented and the bits are spread in a non orthogonal way. Notably, the information bits using the same codebook are defined as a layer, while each layer has a unique sharing pattern of the sub-carrier bands. Namely, the codebook of each layer is different from each other to distinguish the signals overlapping on the same sub-carrier which are generated by the same mother constellation mapping. Then the resultant symbols are modulated and spread by the reference chaotic sequence and its quadrature version generated by Hilbert transform in the time domain, thus the dimension of the constellation could be doubled. Thanks to the sparse spreading, the data from multiple users can overlap and share all the subcarrier bands.

At the SCS-MC-DCSK receiver, reverse operations are conducted. After the Fast Fourier Transform (FFT), the correlated chaotic demodulations are carried out to attain the received information bearing vector. Then we reconstruct the possible transmitted information bearing vector and use a Minimum Distance (MD) detector to identify the layers. Afterwards, for

each layer, the sparse de-spreading is implemented to recover the data for different UEs.

Furthermore, we derive the Pairwise Error Probability (PEP) and the Upper Bound (UB) of the Symbol Error Rate (SER) expression by PEP for the proposed system. Then for the sparse code aided multi-dimension mapping, based on the discrete input constellation, we derive the Constellation Constrained (CC) capacity over the Additive White Gaussian Noise (AWGN) and ergodic CC capacity over the multipath Rayleigh fading channel. Moreover, the energy efficiency, spectrum efficiency and complexity are also analyzed and compared with benchmarks.

Briefly, the main contributions of this paper include:

- 1) We propose to construct the sparse codebook based on the spectrum map, then we group the information bits from different users into multiple layers in a nonorthogonal way, where each layer uses specific subsets of sub-carriers to transmit the signals. Meanwhile, all UEs share the same reference chaotic signal. Thus the spectrum efficiency can be improved by overlapping multiple non-orthogonal layers and orthogonal multiple subcarriers in a subset.
- 2) We propose to modulate the information data with the chaotic sequence and its Hilbert version for each subcarrier. Thus adjacent symbols are extended in the in-phase and quadrature dimensions, accordingly the Euclidean distance could be enlarged and the reliability performances would be enhanced thanks to the shaping gain.
- 3) We propose the receiver architecture for the proposed SCS-MC-DCSK transmitter. After the correlated demodulation with the reference chaotic signal, the MD detection is applied to identify which user equipment the data would be transmitted. Then the sparse de-spreading is conducted to recover the data of each layer.
- 4) We derive the UB of SER performances and the CC capacity of the proposed system over AWGN channel and multipath Rayleigh fading channel with considerations of MUIs. Moreover, the spectrum efficiency as well as the energy efficiency and the computational complexity are analyzed. Simulation results are also provided to validate the theoretical analysis, and to demonstrate the enhanced reliability performances and the anti-jamming capability of our design.

The remainder of the paper is organized as follows. In Section II, the details of the SCS-MC-DCSK transceiver are presented. Section III derives the upper bound of the SER expression and CC capacity over the AWGN channel and multipath Rayleigh fading channel, and analyzes the efficiency as well as the complexity. Subsequently, Section IV provides the simulation results for performance validations and comparisons. Finally, Section V concludes the paper.

II. SCS-MC-DCSK TRANSCEIVER

In this section, the transmitter architecture, the codebook design, the receiver architecture and the MD detector of the proposed SCS-MC-DCSK scheme are presented.

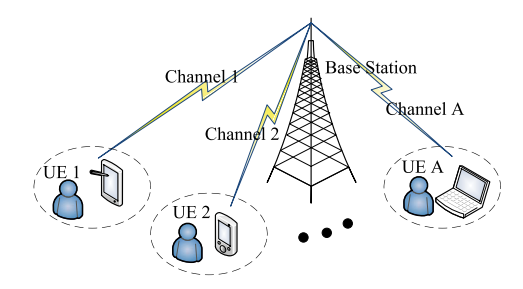


Fig. 1. An example of the uplink multiuser communication scenario using SCS-MC-DCSK transceivers.

Figure 1 illustrates the potential uplink multiuser communication scenario using the proposed SCS-MC-DCSK transceiver, wherein the information bits from multiple UEs with the number of A would be delivered to the Base Station (BS) respectively using predefined sub-bands.

A. Transmitter

As shown in Fig. 2, at the SCS-MC-DCSK transmitter, the bit streams are firstly grouped into layers. Then they are respectively encoded by the sparse code spreader, and modulated by the chaotic sequences and its Hilbert transformation version in the chaos-based spreader. Subsequently, the reference sequence and the information-bearing sequences are transformed by the Inverse Fast Fourier Transform (IFFT) module. Then after the Parallel to Serial (P/S) conversion and adding the Cyclic Prefix (CP), the resultant signals are transmitted over wireless channels. More details are provided as follows.

1) Layering and Sparse Code Spreading: Let $J_a > 0$, $a = 1, \ldots, A$ denote the number of layers used by the UE a and J denote the total number of layers, then we have $\sum_{a=1}^A J_a = J$. In other words, in the proposed system, UE 1, ..., UE A can respectively use J_1, \ldots, J_A layers, which means that each UE could use multiple layers, which are different from the layers used by the other UEs, to deliver the data. When one UE only use one layer, the maximal number of UEs served could be achieved. In this case, J equals to the maximal number of UEs.

To be more explicit, let \mathbf{b}_j $(j=1,\ldots,J)$ denote the information vector of the layer j, which has $log_2(M)$ bits where M represents the size of a codebook. Then \mathbf{b}_j is mapped to \mathbf{X}_j , where the mapping is expressed as $f: \mathbb{B}^{log_2(M)} \to \mathcal{X}_j$, $\mathcal{X}_j \subset \mathbb{C}^{K \times 2}$, $|\mathcal{X}_j| = M$ where the operator $|\cdot|$ represents the evaluation of the size of a set, and K denotes the number of sub-carriers used for transmissions of information bits, which equals to the length of the sparse code. Namely, we have $\mathbf{X}_j = f(\mathbf{b}_j)$.

It's worth pointing out that the sparse code spreading module will spread the signal in the frequency domain and will not add redundant bits. Unlike the error correction coding which lowers the efficiency due to the delivery of redundant bits, thanks to the orthogonality in the time domain brought by the sparse codes, the signals could overlap in an non-orthogonal way, thus the spectrum efficiency could be enhanced. In addition, although the sparse code spreading would not correct

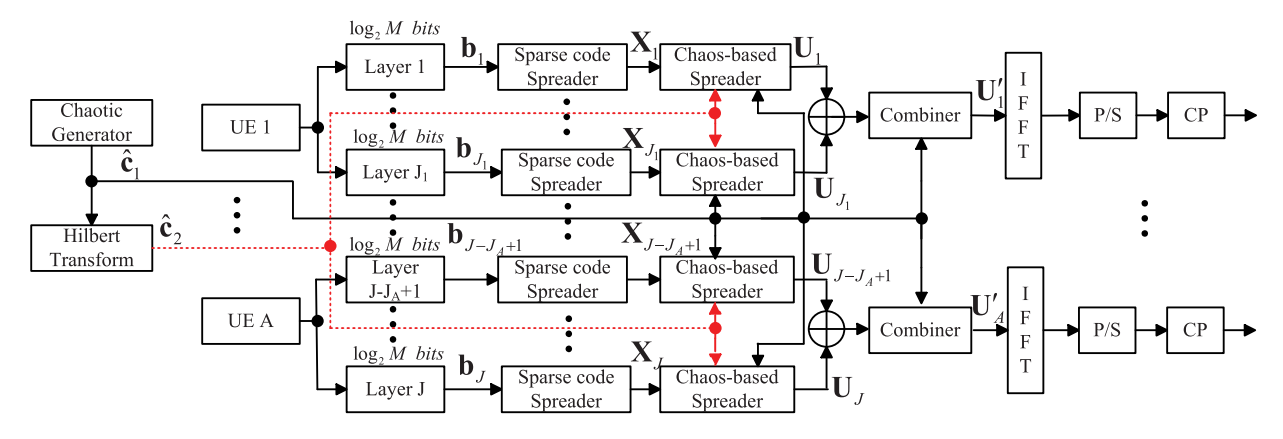


Fig. 2. The SCS-MC-DCSK transmitter structure.

the transmission errors, it could improve the Signal to Noise Ratio (SNR) and thus the reliability performances could be enhanced.

Notably, X_j is a 2K-dimension complex codeword of the layer j's codebook of size M, and is denoted by:

$$\mathbf{X}_{j} = \begin{bmatrix} x_{j,1}, & \dots, & x_{j,K} \\ x_{j,K+1}, & \dots, & x_{j,2K} \end{bmatrix}^{T}, \tag{1}$$

where $\left(\cdot\right)^T$ denote transpose and each column of \mathbf{X}_j represents a sparse complex vector having N < K-nonzero elements, which is equal to the number of the occupied subcarriers by each layer.

2) Chaotic Sequence Generation: On the other hand, the chaotic sequences are generated by the chaotic generator. Let \mathbf{c}_1 denote the chaotic sequence with the length of β , which is generated using the logistic map, i.e., $c_{1,m+1}=1-2c_{1,m}^2$ $(m=1,2,\dots)$, where $c_{1,m}$ is the m_{th} chip of the chaotic sequence. Subsequently, the Hilbert transformation [10] is applied on $\mathbf{c}_1=(c_{1,1},\dots,c_{1,\beta})^T$ and we obtain another quadrature chaotic sequence as $\mathbf{c}_2=(c_{2,1},\dots,c_{2,\beta})^T$. Namely, we have $\sum_{m=1}^{\beta}c_{1,m}c_{2,m}=0$.

We use E_c to represent the energy of \mathbf{c}_1 , namely $E_c = \sum_{m=1}^{\beta} c_{1,m}^2$. Since the Hilbert transformation doesn't change the energy of the sequence, the energy of \mathbf{c}_2 is also E_c . Then we normalize these two chaotic sequences to maintain the energy as 1 to reduce the fluctuations of the energy and reduce the variances. Let $\hat{\mathbf{c}}_1 = \frac{\mathbf{c}_1}{\sqrt{E_c}}$ and $\hat{\mathbf{c}}_2 = \frac{\mathbf{c}_2}{\sqrt{E_c}}$ respectively represent the normalized chaotic sequences, where $\hat{\mathbf{c}}_1 = (\hat{c}_{1,1},\ldots,\hat{c}_{1,\beta})^T$, $\hat{\mathbf{c}}_2 = (\hat{c}_{2,1},\ldots,\hat{c}_{2,\beta})^T$. Then the energy of $\hat{\mathbf{c}}_1$ will be $\sum_{m=1}^{\beta} \hat{c}_{1,m}^2 = \frac{1}{E_c} \sum_{m=1}^{\beta} c_{1,m}^2 = 1$ and so does $\hat{\mathbf{c}}_2$. Notably, after the normalization, the two resultant chaotic sequences still remain orthogonal, i.e. $\sum_{m=1}^{\beta} \hat{c}_{1,m} \hat{c}_{2,m} = 0$.

3) Chaotic Modulation: Next, each row of X_j is respectively modulated with the chaotic sequences $\hat{\mathbf{c}}_1$ and $\hat{\mathbf{c}}_2$. For example, for the k_{th} $(k=1,\ldots,K)$ row of X_j , the chaotic modulated symbol is expressed as:

$$\mathbf{u}_{j,k} = x_{j,k} \hat{\mathbf{c}}_1 + x_{j,K+k} \hat{\mathbf{c}}_2, \quad k = 1, \dots, K.$$
 (2)

Notably, for the K-N zero elements in the column of \mathbf{X}_j , the corresponding elements in the resultant $\mathbf{u}_{j,k}$ are also zero.

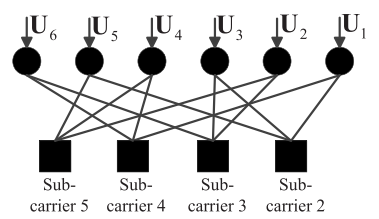


Fig. 3. Factor graph representation, J=6, K=4, N=2 and $d_f=3$.

In addition, the modulated symbols obtained from the j_{th} layer are represented by $\mathbf{U}_j = [\mathbf{u}_{j,1}, \dots, \mathbf{u}_{j,K}]$.

4) Multicarrier Modulation: Subsequently, \mathbf{U}_j from the same UE will be collected and combined with the reference chaotic sequence to constitute the transmitted matrix of each UE. For instance, the matrix of UE 1 is $\mathbf{U}_1' = \sqrt{P} \Big[\mathbf{u}_{ref}, \sum_{j=1}^{J_1} \mathbf{U}_j \Big]$ where P is the energy of transmitted signals and $\mathbf{u}_{ref} = \frac{1}{\sqrt{A}} \hat{\mathbf{c}}_1$. Then, each row of $\mathbf{U}_a'(a=1,\ldots,A)$ is modulated by the IFFT module, the resultant symbols from different UEs are combined and transmitted over wireless channels.

It is worth pointing out that in our design, J layers could share the K sub-carriers with J>K, and each layer occupies N sub-carriers, while the sharing pattern of information-bearing signals is decided by a factor graph matrix denoted by ${\bf F}$ with the size of $K\times J$. If $({\bf F})_{k,j}$, the element of k_{th} row and j_{th} column in ${\bf F}$, has the value of 1, then it means that the layer j uses the $(k+1)_{th}$ sub-carrier. In addition, for those symbols of different layers overlapping over the same one sub-carrier band, we define $d_f=\frac{NJ}{K}$ to denote the number of layers that overlap in one sub-carrier band, and define the overloading factor as $\lambda=J/K$.

For example, Fig. 3 illustrates a factor graph representation \mathbf{F} having 6 layer nodes and 4 sub-carrier nodes. Then we could obtain \mathbf{F} as:

$$\mathbf{F} = \begin{bmatrix} 1 & 0 & 1 & 0 & 1 & 0 \\ 0 & 1 & 1 & 0 & 0 & 1 \\ 1 & 0 & 0 & 1 & 0 & 1 \\ 0 & 1 & 0 & 1 & 1 & 0 \end{bmatrix}. \tag{3}$$

Without loss of generality, we assume that the sub-carrier 1 is used for delivering the reference signal. At the receiver,

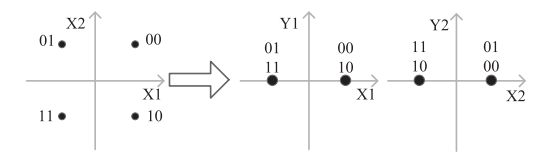


Fig. 4. The mother constellation of the SCS-MC-DCSK system with $J=6,\ M=4,\ K=4,\ N=2.$

the codeword X_j will be used to recover the data of the j_{th} layer from the received overlapped signals. In the following subsection, we will present details about how to construct X_j with the predefined F.

B. Codebook Design

For the proposed system, we propose to construct the codebook with considerations of the spectrum map. More explicitly, we first insert K-N all-zero row vectors into the rows of a unit matrix \mathbf{I}_N based on the factor graph matrix \mathbf{F} to generate a sparse binary mapping matrix \mathbf{V}_j of the layer j. Then we construct the mother constellation map $\mathbf{X}'_j = g(\mathbf{b}_j)$, and the data are modulated with the rotation version of \mathbf{X}'_j . Afterwards, we compose the codeword $\mathbf{X}_j = \mathbf{V}_j (\Delta_j g(\mathbf{b}_j)) = \mathbf{V}_j (\Delta_j \mathbf{X}'_j)$ as the layer j's codebook.

Take (J, M, N, K) = (6, 4, 2, 4) as an example, \mathbf{X}_j would be constructed as follows.

1) Generation of V_j : Let the element "1" denote that the subcarrier is available for the information-bearing sequences of j_{th} layer. For the j_{th} column of F, we insert K-N all-zero row vectors within the rows of a unit matrix I_N to generate V_j . For example, when the first column of F is $(1,0,1,0)^T$, V_1 is expressed as

$$\mathbf{V}_1 = \begin{bmatrix} 1 & 0 & 0 & 0 \\ 0 & 0 & 1 & 0 \end{bmatrix}^T. \tag{4}$$

2) Mother Constellation Mapping $X_j' = g(\mathbf{b}_j)$ and the Constellation Operator Δ_j : Next we would construct the mother constellation and the layer-specific constellation operator. Different from [30], [31], we take the proposed orthogonal chaotic modulation scheme into account of the constellation design. Explicitly, thanks to Hilbert transform, the constellation could be constructed with a matrix with a dimension of 2N. Thus a larger shaping gain [35] could be attained and the reliability performances would be improved.

As shown in Fig. 4, let X1, X2 represent the axis $\hat{\mathbf{c}}_1$ while Y1, Y2 respectively represent the axis $\hat{\mathbf{c}}_2$ of the first and second non-zero element of the codeword. Let the 2N-dimension vector \mathbf{X}'_j represent the mother constellation point corresponding to the information of the layer j, which

is expressed as:

$$\mathbf{X}_{j}' = \begin{bmatrix} x'_{j,1}, \dots, x'_{j,N} \\ x'_{j,N+1}, \dots, x'_{j,2N} \end{bmatrix}^{T}, \tag{5}$$

where the first and second row vectors respectively corresponds to the axes $\hat{\mathbf{c}}_1$ and $\hat{\mathbf{c}}_2$.

Then we rotate \mathbf{X}_j' to generate multiple rotation versions for identifications of different layers at receivers. With considerations of the complexity and the practicality, we propose that the rotation angle keeps the same. Then let $\Delta_j = \left(\Delta^1, \ldots, \Delta^N\right)^T$ denote the constellation rotation operator, we have the n_{th} row of $\Delta_j \mathbf{X}_j'$ as

$$\Delta^{n} (\theta_{1}, \theta_{2}) (x'_{j,n}, x'_{j,n+N})$$

$$= [(x'_{j,n} \cos \theta_{1} - x'_{j,n+N} \sin \theta_{1}),$$

$$(x'_{j,n+N} \cos \theta_{1} + x'_{j,n} \sin \theta_{1})] e^{i\theta_{2}}, \quad n = 1, \dots, N,$$
(6)

where i is the imaginary unit, $\theta_1 = \frac{2\pi}{\rho_1 d_1} (0, \dots, d_1 - 1)$, and $\theta_2 = \frac{2\pi}{\rho_2 d_2} (0, \dots, d_2 - 1)$, which respectively denote the rotation angle in the coordinate constructed by the axes of $\hat{\mathbf{c}}_1$ and $\hat{\mathbf{c}}_2$, and the coordinate constructed by the axes of cosine and sine signals. ρ_1 , ρ_2 are equal to the number of different phases of the points for the practicality, while in this example, $\rho_1 = \rho_2 = 2$, since the constellation for M = 4 only has two phases as shown in Fig. 4. Besides, $d_1 d_2 \geq d_f$, as well as d_1 and d_2 should be as small as possible to enlarge the Euclidian distance between different layers, hence here we set $d_1 = d_2 = 2$.

3) Construction of \mathbf{X}_j : When (J, M, N, K) = (6, 4, 2, 4), we have

$$\Delta_{1} = \begin{bmatrix} \Delta^{1}(0,0) \\ \Delta^{2}(\frac{\pi}{2},0) \end{bmatrix} \quad \Delta_{2} = \begin{bmatrix} \Delta^{1}(0,\frac{\pi}{2}) \\ \Delta^{2}(\frac{\pi}{2},0) \end{bmatrix}
\Delta_{3} = \begin{bmatrix} \Delta^{1}(0,\frac{\pi}{2}) \\ \Delta^{2}(0,0) \end{bmatrix}, \quad \Delta_{4} = \begin{bmatrix} \Delta^{1}(0,0) \\ \Delta^{2}(0,\frac{\pi}{2}) \end{bmatrix}
\Delta_{5} = \begin{bmatrix} \Delta^{1}(\frac{\pi}{2},0) \\ \Delta^{2}(0,0) \end{bmatrix} \quad \Delta_{6} = \begin{bmatrix} \Delta^{1}(\frac{\pi}{2},0) \\ \Delta^{2}(0,\frac{\pi}{2}) \end{bmatrix}. \quad (7)$$

Thus we could obtain \mathbf{X}_{j} using $\mathbf{X}_{j} = \mathbf{V}_{j} \left(\Delta_{j} \mathbf{X}_{j}' \right)$. For example, $\mathbf{X}_{1} = \mathbf{V}_{1} \left(\Delta_{1} \mathbf{X}_{1}' \right) = \begin{bmatrix} x'_{1,1} & 0 - x'_{1,4} & 0 \\ x'_{1,3} & 0 & x'_{1,2} & 0 \end{bmatrix}^{T}$. According to Fig. 4, $x'_{1,3} = x'_{1,4} = 0$, and $x'_{1,1}, x'_{1,2} \in \{\frac{\sqrt{2}}{2}, -\frac{\sqrt{2}}{2}\}$. Referring to Eq. (4), (7) and Fig. 4, Eq. (3) can be rewritten as (8), shown at the bottom of the page.

Then the information-bearing symbols as well as the reference chaotic symbols will be delivered over channels.

$$\begin{bmatrix} x'_{1,1}\hat{\mathbf{c}}_1 & 0 & x'_{3,1}i\hat{\mathbf{c}}_1 & 0 & x'_{5,1}\hat{\mathbf{c}}_2 & 0\\ 0 & x'_{2,1}i\hat{\mathbf{c}}_1 & x'_{3,2}\hat{\mathbf{c}}_1 & 0 & 0 & x'_{6,1}\hat{\mathbf{c}}_2\\ x'_{1,2}\hat{\mathbf{c}}_2 & 0 & 0 & x'_{4,1}\hat{\mathbf{c}}_1 & 0 & x'_{6,2}i\hat{\mathbf{c}}_1\\ 0 & x'_{2,2}\hat{\mathbf{c}}_2 & 0 & x'_{4,2}i\hat{\mathbf{c}}_1 & x'_{5,2}\hat{\mathbf{c}}_1 & 0 \end{bmatrix}.$$
(8)

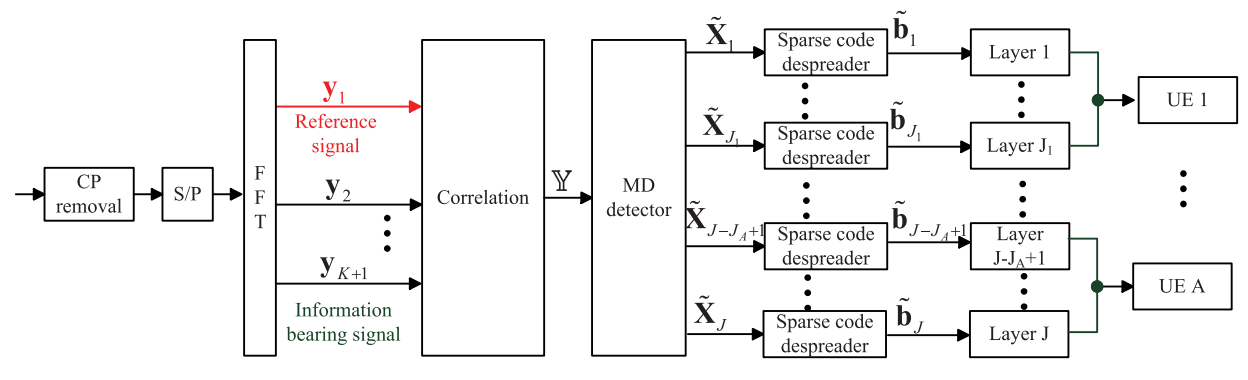


Fig. 5. The block diagram of the SCS-MC-DCSK receiver.

C. Receiver

At the receiver, operations reverse to the transmitter are conducted. After removing the CP and the Serial to Parallel (S/P) conversion, the FFT operations are carried out, then the obtained symbols over the 1_{th} and the $(k+1)_{th}$ $(k=1,\ldots,K)$ sub-carriers undergoing the multiplicative fading and the additive noises are expressed as:

$$\mathbf{y}_{1} = \sum_{a=1}^{A} diag\left(\mathbf{h}_{a,1}\right) \mathbf{u'}_{a,1} + \mathbf{n}_{1},$$

$$\mathbf{y}_{k+1} = \sum_{a=1}^{A} diag\left(\mathbf{h}_{a,k+1}\right) \mathbf{u'}_{a,k+1} + \mathbf{n}_{k+1}, \qquad (9)$$

where \mathbf{y}_1 is the received reference chaotic signal and \mathbf{y}_{k+1} is the received information-bearing signal. The m_{th} $(m=1,\ldots,\beta)$ chip of \mathbf{y}_1 and \mathbf{y}_{k+1} are respectively denoted by $y_{1,m}$ and $y_{k+1,m}$. $\mathbf{u}'_{a,1}$ and $\mathbf{u}'_{a,k+1}$ are respectively 1_{th} and $(k+1)_{th}$ column of \mathbf{U}'_a , $\mathbf{h}_{a,1}$ and $\mathbf{h}_{a,k+1}$ denote the multiplicative complex channel matrix respectively of the 1_{th} and $(k+1)_{th}$ subcarrier and both of the UE a. Both noises \mathbf{n}_1 and \mathbf{n}_{k+1} follow $\mathcal{CN}\left(0,N_0\mathbf{I}\right)$. $diag(\cdot)$ is the diagonal matrix generation operation, where the diagonal element of output matrix corresponds to the entry of the input vector. In addition, $\mathbf{h}_{a,k+1} = \begin{pmatrix} h_{a,k+1,1}, \ldots, h_{a,k+1,\beta} \end{pmatrix}^T$, wherein $h_{a,k+1,m}$ $(m=1,\ldots,\beta)$ represents the coefficient for the $(k+1)_{th}$ subcarrier and m_{th} chip of the UE a, which is given by [26], [36]:

$$h_{a,k+1,m} = \sum_{l=1}^{L} \alpha_{l,\lceil \frac{mT_o}{T_h} \rceil} e^{-2\pi m f_{k+1} \tau_{l,\lceil \frac{mT_o}{T_h} \rceil}}, \qquad (10)$$

where L is the total number of multipath fading channel paths, l is the channel path index, f_{k+1} is the frequency of the $(k+1)_{th}$ sub-carrier, T_o is the OFDM symbol duration while $T_h = qT_o$ is the time duration when the channel coefficient $\alpha_{l,\lceil\frac{mT_o}{T_h}\rceil}$ maintains constant during the transmission of q OFDM symbols. Namely, the parameter q refers to the ratio of the coherence time of the channel to the coherent time of symbols. Besides, $\lceil \cdot \rceil$ is the ceiling operator for rounding up to an integer, and $\tau_{l,\lceil\frac{mT_o}{T_h}\rceil}$ denotes the channel delay of the l_{th} path.

Due to the usage of the CP, in the case that the maximum channel delay time is much lower than the multi-carrier symbol intervals, namely $\tau_{l,\lceil\frac{mT_o}{T_h}\rceil}\ll T_o$, the multipath

interferences at the receiver become negligible, then we have $e^{-2\pi m f_{k+1} au_{l,\lceil \frac{mT_o}{T_h} \rceil}} = e^{-2\pi m (k+1) au_{l,\lceil \frac{mT_o}{T_h} \rceil} / T_o} \approx 1$ [26], [36]. Accordingly, Eq. (10) can be simplified as [26], [36]:

$$h_{a,m} = \sum_{l=1}^{L} \alpha_{l, \lceil \frac{mT_o}{T_h} \rceil}.$$
 (11)

From Eq. (11), it can be seen that $h_{a,m}$ is uncorrelated to the subcarrier index k+1. Then, $\mathbf{h}_{a,k+1}$ can be simplified as $\mathbf{h}_a = (h_{a,1}, \dots, h_{a,m}, \dots, h_{a,\beta})^T$ where $h_{a,m}$ is given in Eq. (11).

In addition, $\mathbf{h}_{a,1} = (h_{a,1,1}, \dots, h_{a,1,\beta})^T$ in Eq. (9) is the coefficient for the 1_{th} subcarrier of the UE a and $h_{a,1,m}$ $(m=1,\dots,\beta)$ is the m_{th} chip of $\mathbf{h}_{a,1}$, denoted by $h_{a,1,m} = \sum_{l=1}^L \alpha_{l,\lceil \frac{m}{q} \rceil} e^{-2\pi m f_1 \tau_{l,\lceil \frac{mT_a}{T_h} \rceil}$. For brevity of expressions, $h_{a,k+1,m}$ is simplified as $h_{a,m}$, while $\mathbf{h}_{a,1}$ is simplified as \mathbf{h}_a .

Without loss of generality, we assume each UE experiences the statistically independent and identically distributed channel conditions. Subsequently, we could retrieve the estimate of $\hat{\mathbf{c}}_1$, $\hat{\mathbf{c}}_2$ denoted by $\tilde{\mathbf{c}}_1 = (\tilde{c}_{1,1}, \dots, \tilde{c}_{1,\beta})^T$,

$$\tilde{c}_{1,m} = \mathcal{R} \left\{ \sqrt{A} \sum_{a=1}^{A} h_{a,m}^* y_{1,m} \right\},$$
(12)

while $\tilde{\mathbf{c}}_2 = (\tilde{c}_{2,1}, \dots, \tilde{c}_{2,\beta})^T$ is obtained by performing Hilbert transform on $\tilde{\mathbf{c}}_1$. Besides, $\mathcal{R}\left\{\cdot\right\}$ takes the real part of a complex number and $(\cdot)^*$ is the conjugate operator.

After the correlated demodulation with $\hat{\mathbf{c}}_1$, $\hat{\mathbf{c}}_2$, we obtain the information-bearing vector as

$$\mathbb{Y} = (\mathbb{Y}_1, \dots, \mathbb{Y}_{4K})^T. \tag{13}$$

The φ_{th} element in \mathbb{Y} is denoted by

$$\mathbb{Y}_{\varphi} = \begin{cases}
\mathcal{R}\left\{\sum_{m=1}^{\beta} \sum_{a_{j} \in \mathcal{A}_{k}} h_{a_{j},m}^{*} y_{k+1,m} \tilde{c}_{1,m}\right\}, \\
\varphi = k \\
\mathcal{I}\left\{\sum_{m=1}^{\beta} \sum_{a_{j} \in \mathcal{A}_{k}} h_{a_{j},m}^{*} y_{k+1,m} \tilde{c}_{1,m}\right\}, \\
\varphi = K + k \\
\mathcal{R}\left\{\sum_{m=1}^{\beta} \sum_{a_{j} \in \mathcal{A}_{k+K}} h_{a_{j},m}^{*} y_{k+1,m} \tilde{c}_{2,m}\right\}, \\
\varphi = 2K + k \\
\mathcal{I}\left\{\sum_{m=1}^{\beta} \sum_{a_{j} \in \mathcal{A}_{k+K}} h_{a_{j},m}^{*} y_{k+1,m} \tilde{c}_{2,m}\right\}, \\
\varphi = 3K + k,
\end{cases} (14)$$

where k = 1, ..., K, $\mathcal{R} \{\cdot\}$ and $\mathcal{I} \{\cdot\}$ respectively take the real part and imaginary part of a complex number and $(\cdot)^*$ is

the conjugate operator. In addition, UE a_j $(a_j \in \{1, ..., A\})$ represents the UE which delivers the information via the j_{th} layer, which constitutes a set $\mathcal{A}_k = \{a_j | x_{j,k} \neq 0\}$. Besides, $h_{a_j,m}$ represents the channel response experienced by the j_{th} layer and the m_{th} chip.

Then the obtained vector is processed by the MD detector to separate symbols to obtain the estimates of the information-bearing symbols $\tilde{\mathbb{X}} = \begin{bmatrix} \tilde{\mathbf{X}}_1, \dots, \tilde{\mathbf{X}}_J \end{bmatrix}$.

Specifically, let \mathbb{Y} denote the received symbol, then the estimate of the codewords $\mathbb{X} = [\mathbf{X}_1, \dots, \mathbf{X}_J]$, which is denoted by $\tilde{\mathbb{X}}$, could be obtained by evaluating the joint optimum Maximum A Posteriori (MAP) as

$$\tilde{\mathbb{X}} = \arg \max_{\mathbb{X} \in \left(\times_{j=1}^{I} \right) \mathcal{X}_{j}} p\left(\mathbb{X} \mid \mathbb{Y} \right), \tag{15}$$

where $\left(\times_{j=1}^{J}\right) \mathcal{X}_{j} = \mathcal{X}_{1} \times \cdots \times \mathcal{X}_{J}$ is the set of transmitted codewords, \times denotes the Cartesian product operator, \mathcal{X}_{j} denotes the set of all the possible \mathbf{X}_{j} .

Furthermore, considering that the MAP method has high complexity due to the probability calculations, we proposed to estimate received symbols by calculating the MD between estimates and received symbols. More explicitly, since the information bits "1" and "0" are uniformly distributed, the information-bearing symbols $\mathbb X$ are also uniformly distributed, hence we have $p(\mathbb X)=\frac{1}{M^J}.$ In addition, using the Gaussian Approximation (GA) methods, we could approximate the elements of $\mathbb Y$ as statistically independent Gaussian random variables. Then according to the Bayes Theorem, i.e. $p\left(\mathbb X\mid \mathbb Y\right)p(\mathbb Y)=p\left(\mathbb Y\mid \mathbb X\right)p(\mathbb X),$ the MAP problem becomes

$$\tilde{\mathbb{X}} = \arg \max_{\mathbb{X} \in \left(\times_{j=1}^{J}\right) \mathcal{X}_{j}} p\left(\mathbb{X} \mid \mathbb{Y}\right) \Leftrightarrow \arg \max_{\mathbb{X} \in \left(\times_{j=1}^{J}\right) \mathcal{X}_{j}} p\left(\mathbb{Y} \mid \mathbb{X}\right)
\Leftrightarrow \arg \max_{\mathbb{X} \in \left(\times_{j=1}^{J}\right) \mathcal{X}_{j}} \frac{\exp\left(-\frac{(\mathbb{Y} - \mathbb{E}[\mathbb{Y}|\mathbb{X}])^{T} \cos[\mathbb{Y}|\mathbb{X}]^{-1} (\mathbb{Y} - \mathbb{E}[\mathbb{Y}|\mathbb{X}])}{2}\right)}{\sqrt{(2\pi)^{4K} \det\left(\cos\left[\mathbb{Y} \mid \mathbb{X}\right]\right)}}
\Leftrightarrow \arg \min_{\mathbb{X} \in \left(\times_{j=1}^{J}\right) \mathcal{X}_{j}} \|\mathbb{Y} - \mathbb{E}\left[\mathbb{Y} \mid \mathbb{X}\right]\|, \tag{16}$$

where $\mathrm{E}[\cdot]$ and $\mathrm{cov}[\cdot]$ respectively denote the numerical expectation and the covariance of the random variable vector, $\det\left(\cdot\right)$ represents the determinant of a matrix, $\left(\cdot\right)^T$ is the transpose operator and $\|\cdot\|$ denotes the Euclidean norm of a vector. In addition, for all $\mathbb{X} \in \left(\times_{j=1}^J\right) \mathcal{X}_j$, since the same transmit power has been applied and the statistical characteristics of channels is assumed to remain the same during the data transmission of a specific user, the influences of $\mathrm{cov}\left[\mathbb{Y} \mid \mathbb{X}\right]$ on the detection performances could be neglected. Therefore, the estimate could be evaluated approximately with the Euclidean norm of $\mathbb{Y} - \mathrm{E}\left[\mathbb{Y} \mid \mathbb{X}\right]$.

After the sparse de-spreading, i.e., $\tilde{\mathbf{b}}_j = f^{-1}(\tilde{\mathbf{X}}_j)$, the estimates from different layers are grouped and delivered to the destination users.

III. THEORETICAL ANALYSIS

In this section, we apply the GA method to analyze the theoretical SER performance, then we analyze the CC capacity, the energy efficiency, the spectrum efficiency and the complexity. A. Expectation and Variance of Received Signals

1) Statistical Characteristics of the Reference Chaotic Signal: Based on Eq. (12), we could rewrite the estimate of the reference chaotic signal $\tilde{c}_{1,m}$ as:

$$\tilde{c}_{1,m} = \sqrt{P} \left| \sum_{a=1}^{A} h_{a,m} \right|^{2} \hat{c}_{1,m} + \mathcal{R} \left\{ \sqrt{A} \sum_{a=1}^{A} h_{a,m}^{*} n_{1,m} \right\}$$

$$= \sqrt{P} \left| \sum_{a=1}^{A} h_{a,m} \right|^{2} \hat{c}_{1,m} + \xi_{m}, \tag{17}$$

where $n_{1,m}$ represents the m_{th} chip of noise imposed on the first sub-carrier and ξ_m represents the noise term of $\tilde{c}_{1,m}$, denoted by $\mathcal{R}\left\{\sqrt{A}\sum_{a=1}^A h_{a,m}^* n_{1,m}\right\}$. $|\cdot|$ represents the absolute value of a scalar.

As mentioned above, the logistic map is applied to generate the chaotic sequence $c_{1,m}$. In this case, we have $\mathrm{E}\left[c_{1,m}^2\right]=\frac{1}{2}$ and $\mathrm{var}\left[c_{1,m}^2\right]=\frac{1}{8}$ [37]. Then for the normalized chaotic sequence $\hat{c}_{1,m}^2$ with the energy equal to $\sum_{m=1}^{\beta}\hat{c}_{1,m}^2=1$, we have

$$E\left[\hat{c}_{1,m}^{2}\right] = \frac{1}{E_{c}} E\left[c_{1,m}^{2}\right] = \frac{1}{2 E_{c}},$$

$$var\left[\hat{c}_{1,m}^{2}\right] = \frac{1}{E_{c}^{2}} var\left[c_{1,m}^{2}\right] = \frac{1}{8E_{c}^{2}}.$$
(18)

The approximate numerical expectation and the variance of \mathcal{E}_m are

$$E\left[\xi_{m} \mid \mathbf{H}\right] = 0, \quad \operatorname{var}\left[\xi_{m} \mid \mathbf{H}\right] = E\left[\xi_{m}^{2} \mid \mathbf{H}\right]$$
$$= \frac{AN_{0}}{2} \left|\sum_{a=1}^{A} h_{a,m}\right|^{2}. \tag{19}$$

where **H** represents the matrix of $[\mathbf{h}_1, \dots, \mathbf{h}_A]$.

Since Hilbert transform would not change the statistical characteristics, we can derive that $\tilde{c}_{2,m}$ has the same conditional numerical expectation and variance as $\tilde{c}_{1,m}$.

2) Numerical Expectation and Variance of Information-Bearing Signals: Based on Eq. (14), we could estimate the expectation and variance of \mathbb{Y} . For different φ , $E[\mathbb{Y}_{\varphi}]$ and $var[\mathbb{Y}_{\varphi}]$ could be evaluated in a similar way. Take \mathbb{Y}_{φ} with $k=1,\cdots,K$ and $\varphi=k$ as an example. We define a set $\mathcal{J}_k=\{j|x_{j,k}\neq 0\}$. With $\tilde{c}_{1,m}$ given by Eq. (17) and $\sum_{m=1}^{\beta}\hat{c}_{1,m}\hat{c}_{2,m}=0$, we could derive \mathbb{Y}_{φ} for $k=1,\cdots,K$ and $\varphi=k$ as (20), shown at the bottom of the next page, where $n_{k+1,m}$ $(k=1,\ldots,K)$ denotes the m_{th} chip of the noise imposed on the $(k+1)_{th}$ sub-carrier. Besides, from Eq. (20), we could see that \mathbb{Y}_{φ} consists of the information-bearing component s_{φ} , and the noisy components $w_{1,\varphi}$, $w_{2,\varphi}$ and $w_{3,\varphi}$.

Next, we evaluate the numerical expectation and the variance of \mathbb{Y}_{φ} . Without loss of generality, we assume the channel response and the energy of the reference chaotic sequence could be learned. Thus for the known E_c and \mathbf{H} , the conditional expectation and the variance of \mathbb{Y}_{φ} are derived as follows:

$$E \left[\mathbb{Y}_{\varphi} \mid \mathbb{X}, \mathbf{H}, E_{c} \right]$$

$$= E \left[s_{\varphi} \mid \mathbb{X}, \mathbf{H}, E_{c} \right] + E \left[w_{1,\varphi} \mid \mathbb{X}, \mathbf{H}, E_{c} \right]$$

$$+ E \left[w_{2,\varphi} \mid \mathbb{X}, \mathbf{H}, E_{c} \right] + E \left[w_{3,\varphi} \mid \mathbb{X}, \mathbf{H}, E_{c} \right],$$

$$\operatorname{var}\left[\mathbb{Y}_{\varphi} \mid \mathbb{X}, \mathbf{H}, E_{c}\right]$$

$$= \operatorname{var}\left[s_{\varphi} \mid \mathbb{X}, \mathbf{H}, E_{c}\right] + \operatorname{var}\left[w_{1,\varphi} \mid \mathbb{X}, \mathbf{H}, E_{c}\right]$$

$$+ \operatorname{var}\left[w_{2,\varphi} \mid \mathbb{X}, \mathbf{H}, E_{c}\right] + \operatorname{var}\left[w_{3,\varphi} \mid \mathbb{X}, \mathbf{H}, E_{c}\right]. \quad (21)$$

Subsequently, we calculate the expectation and the variance of each item in Eq. (21) respectively. First, for the informationbearing item s_{φ} , we have

$$E\left[s_{\varphi}\mid\mathbb{X},\mathbf{H},E_{c}\right]$$

$$=P\sum_{m=1}^{\beta}\mathcal{R}\left\{\left|\sum_{a=1}^{A}h_{a,m}\right|^{2}\left(\sum_{a_{j}\in\mathcal{A}_{k}}h_{a_{j},m}^{*}\right)\sum_{j\in\mathcal{J}_{k}}h_{a_{j},m}x_{j,k}\right\}$$

$$\times E\left[\hat{c}_{1,m}^{2}\right]$$

$$=\frac{P}{2E_{c}}\sum_{m=1}^{\beta}\mathcal{R}\left\{\left|\sum_{a=1}^{A}h_{a,m}\right|^{2}\left(\sum_{a_{j}\in\mathcal{A}_{k}}h_{a_{j},m}^{*}\right)\sum_{j\in\mathcal{J}_{k}}h_{a_{j},m}x_{j,k}\right\},$$

$$var\left[s_{\varphi}\mid\mathbb{X},\mathbf{H},E_{c}\right]$$

$$=P^{2}\sum_{m=1}^{\beta}\mathcal{R}\left\{\left|\sum_{a=1}^{A}h_{a,m}\right|^{2}\left(\sum_{a_{j}\in\mathcal{A}_{k}}h_{a_{j},m}^{*}\right)\sum_{j\in\mathcal{J}_{k}}h_{a_{j},m}x_{j,k}\right\}^{2}$$

$$\times var\left[\hat{c}_{1,m}^{2}\right]$$

$$=\frac{P^{2}}{8E_{c}^{2}}\sum_{m=1}^{\beta}\mathcal{R}\left\{\left|\sum_{a=1}^{A}h_{a,m}\right|^{2}\left(\sum_{a_{j}\in\mathcal{A}_{k}}h_{a_{j},m}^{*}\right)\sum_{j\in\mathcal{J}_{k}}h_{a_{j},m}x_{j,k}\right\}^{2}.$$

$$E\left[s_{\varphi}\mid\mathbb{X},\mathbf{H}\right]$$

$$=\mathcal{R}\left\{P\left|\sum_{a=1}^{A}h_{a}\right|^{2}\left(\sum_{a_{j}\in\mathcal{A}_{k}}h_{a_{j}}^{*}\right)\sum_{j\in\mathcal{J}_{k}}h_{a_{j}}x_{j,k}\right\}$$

$$=\mathcal{R}\left\{P\left|\sum_{a=1}^{A}h_{a}\right|^{2}\left(\sum_{a_{j}\in\mathcal{A}_{k}}h_{a_{j}}^{*}\right)\sum_{j\in\mathcal{J}_{k}}h_{a_{j}}x_{j,k}\right\}^{2}$$

$$\times var\left[\hat{s}_{\varphi}\mid\mathbb{X},\mathbf{H}\right]$$

$$=\mathcal{R}\left\{P\left|\sum_{a=1}^{A}h_{a}\right|^{2}\left(\sum_{a_{j}\in\mathcal{A}_{k}}h_{a_{j}}^{*}\right)\sum_{j\in\mathcal{J}_{k}}h_{a_{j}}x_{j,k}\right\}^{2}$$

$$\times var\left[\hat{s}_{\varphi}\mid\mathbb{X},\mathbf{H}\right]$$

$$=\mathcal{R}\left\{P\left|\sum_{a=1}^{A}h_{a}\right|^{2}\left(\sum_{a_{j}\in\mathcal{A}_{k}}h_{a_{j}}^{*}\right)\sum_{j\in\mathcal{J}_{k}}h_{a_{j}}x_{j,k}\right\}^{2}$$

$$\times var\left[\hat{s}_{\varphi}\mid\mathbb{X},\mathbf{H}\right]$$

$$\times var\left[\hat{s}$$

Considering that $\sum_{m=1}^{\beta} \hat{c}_{1,m}^2 = 1$, we can deduce that $\mathrm{E}\left[\sum_{m=1}^{\beta} \hat{c}_{1,m}^2\right] = 1$ and $\mathrm{var}\left[\sum_{m=1}^{\beta} \hat{c}_{1,m}^2\right] = 0$. In the case that the channel responses remain constant over the whole symbol duration, i.e., $q = \beta$ and $h_{a,m} = h_a$, $h_{a_j,m} = h_{a_j}$, Eq. (22) becomes

$$E\left[s_{\varphi} \mid \mathbb{X}, \mathbf{H}\right]$$

$$= \mathcal{R}\left\{P \middle| \sum_{a=1}^{A} h_{a} \middle|^{2} \left(\sum_{a_{j} \in \mathcal{A}_{k}} h_{a_{j}}^{*}\right) \sum_{j \in \mathcal{J}_{k}} h_{a_{j}} x_{j,k} \right\} E\left[\sum_{m=1}^{\beta} \hat{c}_{1,m}^{2}\right]$$

$$= \mathcal{R}\left\{P \middle| \sum_{a=1}^{A} h_{a} \middle|^{2} \left(\sum_{a_{j} \in \mathcal{A}_{k}} h_{a_{j}}^{*}\right) \sum_{j \in \mathcal{J}_{k}} h_{a_{j}} x_{j,k} \right\},$$

$$\operatorname{var}\left[s_{\varphi} \mid \mathbb{X}, \mathbf{H}\right]$$

$$= \mathcal{R}\left\{P \middle| \sum_{a=1}^{A} h_{a} \middle|^{2} \left(\sum_{a_{j} \in \mathcal{A}_{k}} h_{a_{j}}^{*}\right) \sum_{j \in \mathcal{J}_{k}} h_{a_{j}} x_{j,k} \right\}^{2}$$

$$\times \operatorname{var}\left[\sum_{a=1}^{\beta} \hat{c}_{1,m}^{2}\right] = 0. \tag{23}$$

$$\mathbb{Y}_{\varphi} = \mathcal{R} \Big\{ \sum_{m=1}^{\beta} \sum_{a_{j} \in \mathcal{A}_{k}} h_{a_{j},m}^{*} y_{k+1,m} \tilde{c}_{1,m} \Big\} \\
= \mathcal{R} \Big\{ \sum_{m=1}^{\beta} \Big(\sum_{a_{j} \in \mathcal{A}_{k}} h_{a_{j},m}^{*} \Big) \Big(\sum_{j \in \mathcal{J}_{k}} h_{a_{j},m} \sqrt{P} x_{j,k} \hat{c}_{1,m} \\
+ \sum_{j \in \mathcal{J}_{k+K}} h_{a_{j},m} \sqrt{P} x_{j,k+K} \hat{c}_{2,m} + n_{k+1,m} \Big) \Big(\sqrt{P} \Big| \sum_{a=1}^{A} h_{a,m} \Big|^{2} \hat{c}_{1,m} + \xi_{m} \Big) \Big\} \\
= \mathcal{R} \Big\{ P \sum_{m=1}^{\beta} \Big| \sum_{a=1}^{A} h_{a,m} \Big|^{2} \Big(\sum_{a_{j} \in \mathcal{A}_{k}} h_{a_{j},m}^{*} \Big) \sum_{j \in \mathcal{J}_{k}} h_{a_{j},m} x_{j,k} c_{1,m}^{2} \Big\} \\
+ \mathcal{R} \Big\{ \sqrt{P} \sum_{m=1}^{\beta} \Big| \sum_{a=1}^{A} h_{a,m} \Big|^{2} \Big(\sum_{a_{j} \in \mathcal{A}_{k}} h_{a_{j},m}^{*} \Big) \hat{c}_{1,m} n_{k+1,m} \Big\} \\
+ \mathcal{R} \Big\{ P \sum_{m=1}^{\beta} \Big| \sum_{a=1}^{A} h_{a,m} \Big|^{2} \Big(\sum_{a_{j} \in \mathcal{A}_{k}} h_{a_{j},m}^{*} \Big) \sum_{j \in \mathcal{J}_{k+K}} h_{a_{j},m} x_{j,k+K} \hat{c}_{1,m} \hat{c}_{2,m} \Big\} \\
= 0 \\
+ \mathcal{R} \Big\{ \sum_{m=1}^{\beta} \Big(\sum_{a_{j} \in \mathcal{A}_{k}} h_{a_{j},m}^{*} \Big) n_{k+1,m} \xi_{m} \Big\} \\
+ \mathcal{R} \Big\{ \sum_{m=1}^{\beta} \Big(\sum_{a_{j} \in \mathcal{A}_{k}} h_{a_{j},m}^{*} \Big) \Big(\sum_{j \in \mathcal{J}_{k}} h_{a_{j},m} \sqrt{P} x_{j,k} \hat{c}_{1,m} + \sum_{j \in \mathcal{J}_{k+K}} h_{a_{j},m} \sqrt{P} x_{j,k+K} \hat{c}_{2,m} \Big) \xi_{m} \Big\}, \tag{20}$$

Thus we obtain:

$$E[\mathbb{Y}_{\varphi} \mid \mathbb{X}, \mathbf{H}, E_c] = E[s_{\varphi} \mid \mathbb{X}, \mathbf{H}, E_c]. \tag{24}$$

On the other hand, the variance of $w_{1,\varphi}$, $w_{2,\varphi}$ and $w_{3,\varphi}$ could also be derived as:

$$\operatorname{var}\left[w_{1,\varphi}\mid\mathbb{X},\mathbf{H},E_{c}\right]$$

$$=\frac{PN_{0}}{4E_{c}}\sum_{m=1}^{\beta}\left|\sum_{a=1}^{A}h_{a,m}\right|^{4}\left|\sum_{a_{j}\in\mathcal{A}_{k}}h_{a_{j},m}\right|^{2},$$

$$\operatorname{var}\left[w_{2,\varphi}\mid\mathbb{X},\mathbf{H},E_{c}\right]$$

$$=\frac{AN_{0}^{2}}{4}\sum_{m=1}^{\beta}\left|\sum_{a=1}^{A}h_{a,m}\right|^{2}\left|\sum_{a_{j}\in\mathcal{A}_{k}}h_{a,m}\right|^{2},$$

$$\operatorname{var}\left[w_{3,\varphi}\mid\mathbb{X},\mathbf{H},E_{c}\right]$$

$$=\frac{APN_{0}}{4E_{c}}\sum_{m=1}^{\beta}\left|\sum_{a=1}^{A}h_{a,m}\right|^{2}\left\{\mathcal{R}\left\{\left(\sum_{a_{j}\in\mathcal{A}_{k}}h_{a_{j},m}^{*}\right)\right\}\right\}$$

$$\times\sum_{j\in\mathcal{J}_{k}}h_{a_{j},m}x_{j,k}\right\}^{2}+\mathcal{R}\left\{\left(\sum_{a_{j}\in\mathcal{A}_{k}}h_{a_{j},m}^{*}\right)\right\}$$

$$\times\sum_{j\in\mathcal{J}_{k}}h_{a_{j},m}x_{j,k+K}\right\}^{2}.$$
(25)

Substituting Eq. (22), (25) into (21), we can obtain the $var[Y_{\varphi} \mid X, H, E_c]$.

Similarly, for the other $\varphi = K + k$, 2K + k, 3K + k, we could derive $\operatorname{var}\left[\mathbb{Y}_{\varphi} \mid \mathbb{X}, \mathbf{H}, E_{c}\right]$ and $\operatorname{E}\left[\mathbb{Y}_{\varphi} \mid \mathbb{X}, \mathbf{H}, E_{c}\right]$ as similar methods.

B. SER Analysis

Considering the decision making is based on a decision cell of a multidimensional signal point and thus only the PEP could be determined explicitly, hence in the following SER analysis, we derive the union bound based on the PEP.

According to Eq. (16) and Eq. (24), the estimates of \mathbb{X} could be obtained by

$$\widetilde{\mathbb{X}} \approx \arg\min_{\mathbb{X} \in (\times_{i-1}^{\mathcal{X}}) \mathcal{X}_i} \| \mathbb{Y} - \mathbb{E} \left[\mathbf{s} \mid \mathbb{X}, \mathbf{H}, E_c \right] \|, \tag{26}$$

where $\mathbf{s} = (s_1, \dots, s_{\varphi}, \dots, s_{4K})^T$.

As shown in Eq. (22), the evaluation of $\mathrm{E}\left[s_{\varphi}\mid\mathbb{X},\mathbf{H},E_{c}\right]$ requires the known E_{c} , which could be delivered via the dedicated control channel or be approximately calculated via the numerical average value. With considerations that $\mathrm{E}\left[E_{c}\right]=\beta\mathrm{E}\left[c_{1,m}^{2}\right]=\frac{\beta}{2}$, we could obtain the approximate value of $\mathrm{E}\left[\mathbf{s}\mid\mathbb{X},\mathbf{H},E_{c}\right]$, which is denoted by \mathbb{S} . Accordingly, Eq. (26) becomes

$$\tilde{\mathbb{X}} \approx \arg \min_{\mathbb{X} \in \left(\times_{j=1}^{J} \right) \mathcal{X}_{j}} \| \mathbb{Y} - \mathbb{S} \|.$$
 (27)

Next, we derive the PEP. Let $PEP\left(\mathbb{X} \to \mathbb{X} \mid \mathbf{H}, E_c\right)$ represent the PEP of mistaking \mathbb{X} for \mathbb{X} with the known \mathbf{H} and E_c , where $\mathbb{X} \in \left(\times_{j=1}^J\right) \mathcal{X}_j$, $\mathbb{X} \in \mathbb{C}_{\left(\times_{j=1}^J\right) \mathcal{X}_j} \mathbb{X}$, and $\mathbb{C}_{\left(\times_{j=1}^J\right) \mathcal{X}_j} \mathbb{X}$ denotes the set of all the possible error symbols and \mathbb{C} is the operator of the complementary set. Then, the average PEP can

be derived by averaging conditional PEP over the distribution of ${\bf H}$ and E_c as:

$$\overline{PEP}\left(\mathbb{X} \to \mathring{\mathbb{X}}\right) = \mathbb{E}\left[PEP\left(\mathbb{X} \to \mathring{\mathbb{X}} \mid \mathbf{H}, E_c\right)\right].$$
 (28)

According to Eq. (27), we could observe that when $\|\mathbb{Y} - \mathbb{S}\| > \|\mathbb{Y} - \hat{\mathbb{S}}\|$, the symbol decision error will occur. Then we could derive the PEP as follows:

$$PEP\left(\mathbb{X} \to \dot{\mathbb{X}} \mid \mathbf{H}, E_c\right) = p\left(\|\mathbb{Y} - \mathbb{S}\| > \|\mathbb{Y} - \dot{\mathbb{S}}\| \mid \mathbf{H}, E_c\right). \tag{29}$$

Then the inequality of $\|\mathbb{Y} - \mathbb{S}\| > \|\mathbb{Y} - \grave{\mathbb{S}}\|$ can be equivalently evaluated by:

$$\|\mathbb{Y} - \mathbb{S}\|$$

$$> \|\mathbb{Y} - \dot{\mathbb{S}}\| \Leftrightarrow \|\mathbb{Y} - \mathbb{S}\|^{2} > \|\mathbb{Y} - \dot{\mathbb{S}}\|^{2}$$

$$\Leftrightarrow \|\mathbb{Y} - \mathbb{S}\|^{2} > \|\mathbb{Y} - \mathbb{S} + \mathbb{S} - \dot{\mathbb{S}}\|^{2}$$

$$\Leftrightarrow \|\mathbb{Y} - \mathbb{S}\|^{2} > \|\mathbb{Y} - \mathbb{S}\|^{2} + 2(\mathbb{S} - \dot{\mathbb{S}})^{T} (\mathbb{Y} - \mathbb{S}) + \|\mathbb{S} - \dot{\mathbb{S}}\|^{2}$$

$$\Leftrightarrow (\mathbb{S} - \dot{\mathbb{S}})^{T} (\mathbb{Y} - \mathbb{S}) < -\frac{\|\mathbb{S} - \dot{\mathbb{S}}\|^{2}}{2}$$

$$\Leftrightarrow (\mathbb{S} - \dot{\mathbb{S}})^{T} (\mathbb{Y} - \mathbb{S}) + (\mathbb{S} - \dot{\mathbb{S}})^{T} (\mathbb{S} - \mathbb{E} [\mathbb{Y} \mid \mathbb{X}, \mathbf{H}, E_{c}])$$

$$< -\frac{\|\mathbb{S} - \dot{\mathbb{S}}\|^{2}}{2} + (\mathbb{S} - \dot{\mathbb{S}})^{T} (\mathbb{S} - \mathbb{E} [\mathbb{Y} \mid \mathbb{X}, \mathbf{H}, E_{c}])$$

$$\Leftrightarrow (\mathbb{S} - \dot{\mathbb{S}})^{T} (\mathbb{Y} - \mathbb{E} [\mathbb{Y} \mid \mathbb{X}, \mathbf{H}, E_{c}])$$

$$< -\frac{\|\mathbb{S} - \dot{\mathbb{S}}\|^{2}}{2} + (\mathbb{S} - \dot{\mathbb{S}})^{T} (\mathbb{S} - \mathbb{E} [\mathbb{Y} \mid \mathbb{X}, \mathbf{H}, E_{c}]). \tag{30}$$

Using the GA method, $(\mathbb{S} - \dot{\mathbb{S}})^T (\mathbb{Y} - \mathbb{E} [\mathbb{Y} \mid \mathbb{X}, \mathbf{H}, E_c])$ can be treated as a gaussian random variable with the expectation of zero and the variance of $(\mathbb{S} - \dot{\mathbb{S}})^T \text{cov} [\mathbb{Y} \mid \mathbb{X}, \mathbf{H}, E_c] (\mathbb{S} - \dot{\mathbb{S}})$.

Then we obtain the expression of the conditional PEP as:

$$PEP\left(\mathbb{X} \to \dot{\mathbb{X}} \mid \mathbf{H}, E_{c}\right)$$

$$= Q\left(\frac{\left\|\mathbb{S} - \dot{\mathbb{S}}\right\|^{2} + 2\left(\mathbb{S} - \dot{\mathbb{S}}\right)^{T} \left(\mathbb{E}\left[\mathbb{Y} \mid \mathbb{X}, \mathbf{H}, E_{c}\right] - \mathbb{S}\right)}{2\sqrt{\left(\mathbb{S} - \dot{\mathbb{S}}\right)^{T} \cos\left[\mathbb{Y} \mid \mathbb{X}, \mathbf{H}, E_{c}\right] \left(\mathbb{S} - \dot{\mathbb{S}}\right)}}\right),$$
(31)

where Q(x) is the complementary cumulative distribution function of a standard normally distributed random variable, which is expressed as $Q(x) = \int_x^{+\infty} \frac{1}{\sqrt{2\pi}} \exp\left(-\frac{1}{2}t^2\right) dt$. cov $[\mathbb{Y} \mid \mathbb{X}, \mathbf{H}, E_c]$ is a diagonal matrix and the diagonal element is the variance of \mathbb{Y}_{φ} . Note that the item $\|\mathbb{S} - \hat{\mathbb{S}}\|$ calculates the errors of the estimates induced by imperfect transmissions including the non-orthogonal sparse code, the fading fading and noises etc. Moreover, since in Eq. (31), there are multiple random variables so that the calculation of the expectation in Eq. (28) is a multiple integration which can be evaluated approximately by applying the Monte Carlo integration method [38] as:

$$\overline{PEP}\left(\mathbb{X} \to \mathring{\mathbb{X}}\right) = \frac{1}{\chi} \sum_{n=1}^{\chi} \left(PEP_n\left(\mathbb{X} \to \mathring{\mathbb{X}} \mid \mathbf{H}, E_c\right)\right),\tag{32}$$

where χ denotes the number of trials.

Finally, we can derive the union upper bound of the SER as [39]:

$$SER \leq \frac{1}{M^{J}} \sum_{\mathbb{X} \in \left(\times_{j=1}^{J}\right) \mathcal{X}_{j}} \left(\sum_{\mathring{\mathbb{X}} \in \mathbb{C}_{\left(\times_{j=1}^{J}\right) \mathcal{X}_{j}} \mathbb{X}} \overline{PEP} \left(\mathbb{X} \to \mathring{\mathbb{X}}\right) \right).$$
(33)

C. Capacity Analysis

The CC capacity is measured by the mutual information between the input and the output, where the input belongs to a finite set $(\times_{j=1}^J) \mathcal{X}_j$ and is uniformly distributed. Then we calculate $I(\mathbb{X}:\mathbb{Y})$ as:

$$I(X:Y) = H(Y) - H(Y \mid X), \tag{34}$$

where $H(\mathbb{Y})$ is given by $H(\mathbb{Y}) = -\int p(\mathbb{Y}) \log_2(p(\mathbb{Y})) d\mathbb{Y}$ where \mathbb{Y} is a vector with the length of 4K and thus

$$\int d\mathbb{Y} = \underbrace{\int \cdots \int}_{4K} d\mathbb{Y}_1 \cdots d\mathbb{Y}_{4K}.$$
 (35)

Since \mathbb{X} is uniformly distributed, we have $p(\mathbb{X}) = \frac{1}{M^J}$. $p(\mathbb{Y})$ would be calculated by:

$$p(\mathbb{Y}) = \sum_{\mathbb{X} \in \left(\times_{j=1}^{J}\right) \mathcal{X}_{j}} p(\mathbb{X}) p(\mathbb{Y} \mid \mathbb{X})$$

$$= \frac{1}{M^{J}} \sum_{\mathbb{X} \in \left(\times_{j=1}^{J}\right) \mathcal{X}_{j}} p(\mathbb{Y} \mid \mathbb{X}). \tag{36}$$

Then we could evaluate $H(\mathbb{Y})$ by:

$$\begin{split} &H\left(\mathbb{Y}\right) \\ &= -\int p\left(\mathbb{Y}\right)\log_{2}\left(\frac{1}{M^{J}}\sum_{\mathbb{X}\in\left(\times_{j=1}^{J}\right)\mathcal{X}_{j}}p\left(\mathbb{Y}\mid\mathbb{X}\right)\right)d\mathbb{Y} \\ &= -\int p\left(\mathbb{Y}\right)\left[\log_{2}\left(\sum_{\mathbb{X}\in\left(\times_{j=1}^{J}\right)\mathcal{X}_{j}}p\left(\mathbb{Y}\mid\mathbb{X}\right)\right) - \log_{2}\left(M^{J}\right)\right]d\mathbb{Y} \\ &= \log_{2}\left(M^{J}\right) \end{split}$$

$$-\frac{1}{M^{J}} \sum_{\mathbb{X}'' \in \left(\times_{j=1}^{J}\right) \mathcal{X}_{j}} \int p\left(\mathbb{Y} \mid \mathbb{X}''\right)$$

$$\times \log_{2} \left(\sum_{\mathbb{X} \in \left(\times_{j=1}^{J}\right) \mathcal{X}_{j}} p\left(\mathbb{Y} \mid \mathbb{X}\right)\right) d\mathbb{Y}. \tag{37}$$

On the other hand, $H(\mathbb{Y} \mid \mathbb{X})$ in Eq. (34) can be calculated by:

$$H\left(\mathbb{Y}\mid\mathbb{X}\right) = \sum_{\mathbb{X}''\in\left(\times_{j=1}^{J}\right)\mathcal{X}_{j}} p\left(\mathbb{X}\right)H\left(\mathbb{Y}\mid\mathbb{X}''\right) = -\frac{1}{M^{J}} \sum_{\mathbb{X}''\in\left(\times_{j=1}^{J}\right)\mathcal{X}_{j}} \int p\left(\mathbb{Y}\mid\mathbb{X}''\right)\log_{2}\left(p\left(\mathbb{Y}\mid\mathbb{X}''\right)\right)d\mathbb{Y}.$$
(38)

Using the GA method, $p(Y \mid X)$ is derived as (39), shown at the bottom of the page.

With the aid of Eq. (37), (38) and (39), we can calculate the CC as (40), shown at the bottom of the page.

Then, substituting the numerical expectation and covariance of \mathbb{Y} obtained in subsection III-A into Eq. (40), we can calculate the ergodic CC capacity over the multipath Rayleigh fading channel using Monte Carlo integration method.

D. Energy Efficiency Analysis

The definition of the energy efficiency is given by [25], [26]

$$\Psi = \frac{E_{information}}{E_b},\tag{41}$$

where $E_{information}$ is the energy of the information-bearing signal and E_b represents the transmitted energy for each bit. Note that the bit energy satisfies $E_b = E_{reference} + E_{information}$ and the reference signal energy is $E_{reference} = \frac{1}{\lambda K} E_{information}$. For the proposed scheme where K is the number of the subcarriers for information-bearing signal and $\lambda = \frac{J}{K}$ denotes the overloading factor. We use K_{all} to denote the number of all subcarriers and thus, $K_{all} = K + 1$ for our scheme. Therefore, the energy efficiency of SCS-MC-DCSK is $\Psi = \frac{\lambda(K_{all}-1)}{\lambda(K_{all}-1)+1}$.

$$p(\mathbb{Y} \mid \mathbb{X}) = \mathbb{E}\left[p(\mathbb{Y} \mid \mathbb{X}, \mathbf{H}, E_{c})\right]$$

$$= \mathbb{E}\left[\frac{\exp\left(-\frac{(\mathbb{Y} - \mathbb{E}[\mathbb{Y} \mid \mathbb{X}, \mathbf{H}, E_{c}])^{T} \cos(\mathbb{Y} \mid \mathbb{X}, \mathbf{H}, E_{c}]^{-1}(\mathbb{Y} - \mathbb{E}[\mathbb{Y} \mid \mathbb{X}, \mathbf{H}, E_{c}])}{\sqrt{(2\pi)^{4K} \det\left(\cos\left[\mathbb{Y} \mid \mathbb{X}, \mathbf{H}, E_{c}\right]\right)}}\right]. \tag{39}$$

$$I(\mathbb{X} : \mathbb{Y}) = H(\mathbb{Y}) - H(\mathbb{Y} \mid \mathbb{X}) = \log_{2}\left(M^{J}\right) - \frac{1}{M^{J}} \sum_{\mathbb{X}'' \in \left(\times_{j=1}^{J}\right) \mathcal{X}_{j}} \times \mathbb{E}\left[\log_{2}\left(\frac{\sum_{\mathbb{X} \in \left(\times_{j=1}^{J}\right) \mathcal{X}_{j}} \exp\left(-\frac{(\mathbb{Y} - \mathbb{E}[\mathbb{Y} \mid \mathbb{X}, \mathbf{H}, E_{c}])^{T} \cos(\mathbb{Y} \mid \mathbb{X}, \mathbf{H}, E_{c}]^{-1}(\mathbb{Y} - \mathbb{E}[\mathbb{Y} \mid \mathbb{X}, \mathbf{H}, E_{c}])}{2}\right)}{\exp\left(-\frac{(\mathbb{Y} - \mathbb{E}[\mathbb{Y} \mid \mathbb{X}'', \mathbf{H}, E_{c}])^{T} \cos(\mathbb{Y} \mid \mathbb{X}'', \mathbf{H}, E_{c}]^{-1}(\mathbb{Y} - \mathbb{E}[\mathbb{Y} \mid \mathbb{X}'', \mathbf{H}, E_{c}])}}{2}\right)\right]. \tag{40}$$

TABLE I ENERGY EFFICIENCY COMPARISON

Scheme	SCS-MC-DCSK	DCSK [4]	MU-MC-DCSK [25]
Ψ	$\frac{\lambda(K_{all}-1)}{\lambda(K_{all}-1)+1}$	$\frac{1}{2}$	$\frac{K_{all}-A}{K_{all}}$
Scheme	MU-OFDM-DCSK [26]	SCMA [34]	
Ψ	$\frac{K_{all}-A}{K_{cu}+1-A}$	1	

TABLE II SPECTRUM EFFICIENCY COMPARISON

Scheme	SCS-MC-DCSK	MU-MC-DCSK [25]
η	$\frac{\lambda(K_{all}-1)\log_2 M}{\beta K_{all}}$	$\frac{K_{all}-A}{\beta K_{all}}$
Scheme	MU-OFDM-DCSK [26]	SCMA [34]
η	$\frac{(K_{all}-A)A}{\beta K_{all}}$	$\frac{\lambda K_{all} \log_2 M}{K_{all}}$

Then, we compare the energy efficiency of the proposed scheme with the counterpart schemes including DCSK [4], MU-MC-DCSK [25], MU-OFDM-DCSK [26] and SCMA [34] in TABLE I. For fairness of the comparison, we assume that in these schemes, the reference chaotic signal of each UE will occupy only one subcarrier. It could be observed from TABLE I that when $\lambda = \frac{J}{K_{all}-1} > 1 \ge \frac{K_{all}-A}{K_{all}-1}$, our proposed scheme can achieve the higher energy efficiency compared with DCSK [4], MU-MC-DCSK [25] and MU-OFDM-DCSK [26]. In addition, we can see that the energy efficiency of SCMA [34] without reference signals is 1, while the efficiency of our scheme approaches 1 as J becomes larger.

E. Spectrum Efficiency Analysis

According to the definition of the spectrum efficiency [23], which is the ratio of the bit rate to the total bandwidth, the spectrum efficiency of the SCS-MC-DCSK scheme is derived as below:

$$\eta = \frac{\frac{J \log_2 M}{\beta T_o}}{B_c K_{all}} = \frac{\lambda \left(K_{all} - 1\right) \log_2 M}{\beta K_{all}},\tag{42}$$

where η represents the spectrum efficiency, β is the length of the chaotic sequence and $\log_2 M$ is the number of modulated bits transmitted via each layer, M is the size of a codebook, T_o denotes the duration of each chaotic chip (which is equal to the OFDM symbol duration in this paper), thus βT_o represents the symbol duration. In addition, $B_c = 1/T_o$ represents the bandwidth occupied by each subcarrier under the assumption of the perfect filtering.

Note that although multiple zeros are inserted to generate the codebook, no redundant bits are added and thus the spectrum efficiency will not be lowered by the sparse code spreading. Instead, thanks to non orthogonal multiplexing of layers, the signals could overlap to deliver the information and thus the spectrum efficiency can be improved.

As shown in TABLE II, we can observe that the presented SCS-MC-DCSK scheme achieves larger spectrum efficiency than the MU-MC-DCSK [25]. As to the MU-OFDM-DCSK system [26], the spectrum efficiency performance is dependent on the value of the parameter. More explicitly, when

TABLE III
COMPLEXITY COMPARISON

Scheme	SCS-MC-DCSK	MU-MC-DCSK [25]	MU-OFDM-DCSK [26]
$\mathcal{O}\left(\cdot\right)$	$\mathcal{O}\left(M^{\lambda K}\right)$	$\mathcal{O}\left(K+1-A\right)$	$\mathcal{O}\left(\left(K+1-A\right)A\right)$

TABLE IV
PARAMETER SETTINGS

Value
2, 3, 4, 6
5
1, 2, 4, 6
4
4
2
64, 128, 256, 512
8, 16, 32, 128
AWGN,
multipath Rayleigh fading
$\frac{1}{2}, \frac{1}{3}, \frac{1}{6}$

 $\lambda\left(K_{all}-1\right)\log_{2}M=J\log_{2}M>\left(K_{all}-A\right)A$, the proposed system can achieve larger spectrum efficiency than the MU-OFDM-DCSK system [26]. In addition, we can also notice that since SCMA systems need not to deliver reference signals, the spectrum efficiency is slightly higher than our proposed scheme.

F. Complexity Analysis

As mentioned above, in the proposed scheme, we use the MD detector at the receiver to demodulate the signals, which requires to traverse $M^{\lambda K}=M^J$ possible transmitted symbols. Thus, the complexity is $\mathcal{O}\left(M^{\lambda K}\right)$. For the benchmark schemes MU-MC-DCSK [25] and MU-OFDM-DCSK [26], since the subcarrier-wise demodulation is conducted, the traversal time would be shorter.

As shown in TABLE III, our proposed scheme has relatively higher complexity. Since we propose to apply our design in the uplink scenario as shown in Fig. 1, the complexity is acceptable for the base station which usually has high computational capabilities.

IV. SIMULATION RESULTS

In this section, simulation results are given to evaluate the performances of the proposed SCS-MC-DCSK scheme.

The parameters are set as the same as those used in the mother constellations shown in Fig. 4 and the factor graph given in Eq. (8), which is shown in TABLE IV. Besides, as shown in Eq. (11), we use $\alpha_{l,\lceil\frac{mT_o}{T_h}\rceil}$ to represent the channel coefficient of the l_{th} path.

Notably, if A > 1, UEs will share the available layers fairly with equally allocated layers. Besides, the same one reference chaotic sequence is shared by different users for higher spectrum efficiency.

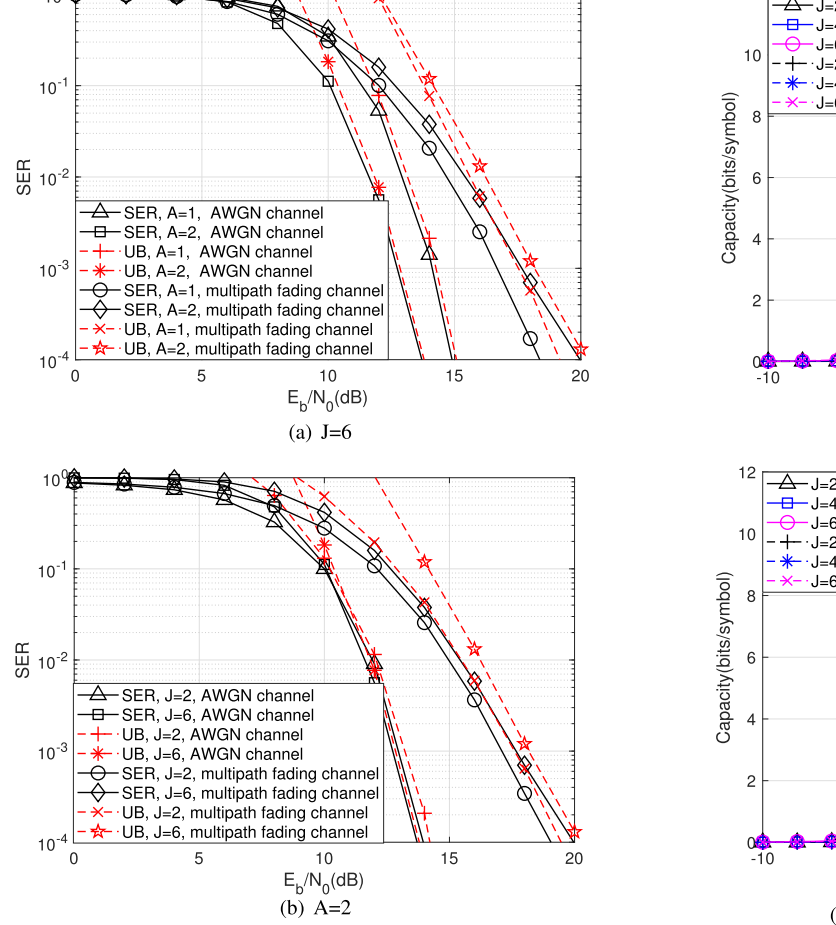


Fig. 6. Comparisons of the simulated SER and the theoretical UB of the SCS-MC-DCSK with $\beta=128$.

A. Theoretical SER UB and Simulated Performances

Considering that different number of layers and UEs would induce different interferences due to the non-orthogonality of sparse codes, Fig. 6(a) and Fig. 6(b) respectively compare the simulated SER of SCS-MC-DCSK and the numerical UB over the AWGN channel and the multipath fading channel when the number of layers J or UEs A is different. The multipath fading channel used in Fig. 6 is a three-path Rayleigh fading channel with q=16.

We can observe from these two figures that the theoretical upper bounds are tight for large E_b/N_0 . We could also notice that in Fig. 6(a), with larger number of UEs of A = 2, the SER performances would not degrade over AWGN channel but aggravate over multipath fading channels. In addition, from Fig. 6(b), we could see that larger number of layers would degrade the SER performances no matter over AWGN channel or the multipath fading channel. The reason is that for AWGN channel, when A increases, no additional phase rotation is introduced, hence the Euclidean distances between adjacent symbols would not be shortened. By contrast, due to the fading and the overlapping, the signals would undergo the phase distortions, thereby leading to the shorter Euclidean distances. As a result, SER performances of the proposed system degrade with a larger number of UEs over fading channels or a larger number of layers for different channels.

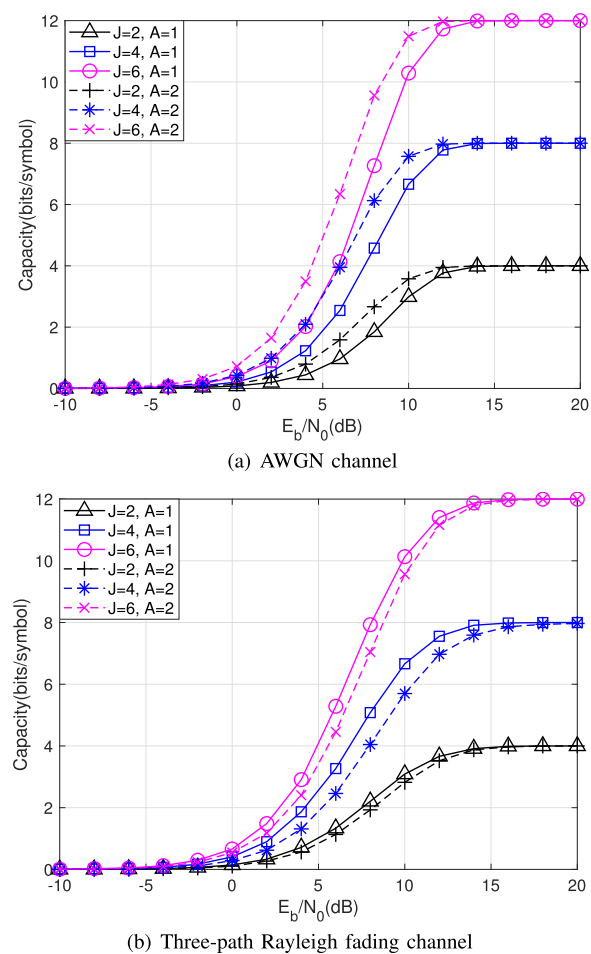


Fig. 7. The CC capacity of the SCS-MC-DCSK system with $\beta = 128$.

Moreover, as seen in Fig. 6(a), for J=6, the SER performances with A=1 are worse than those with A=2 over the AWGN channel. The reason is that when A=2, two same reference chaotic signals used by two UEs could be combined to enhance the SNR by exploiting the diversity gain. In addition, from Fig. 6(b), we can notice that for AWGN channel, when E_b/N_0 is larger than about 12dB, the system with J=6 would provide better SER performances. The reason is that when J and E_b/N_0 has a larger value, the symbol energy $E_{symbol}=JE_b\log_2 M$ will also increase, thus the SER performances could be improved.

B. Capacity Performance

Figure 7(a) and Fig. 7(b) respectively analyze the CC capacity of the proposed system with different J and A over the AWGN channel and the three-path Rayleigh fading channel with q=16. We can observe that for both channels, when the number of layers J increases from 2 to 6, the CC capacity will increase accordingly since more bits could be delivered via different layers.

Additionally, as shown in Fig. 7(a), the CC capacity of the system with A=2 is obviously larger than that with A=1. The reason is that the diversity gain brought by delivering the same reference chaotic signals of different UEs improve

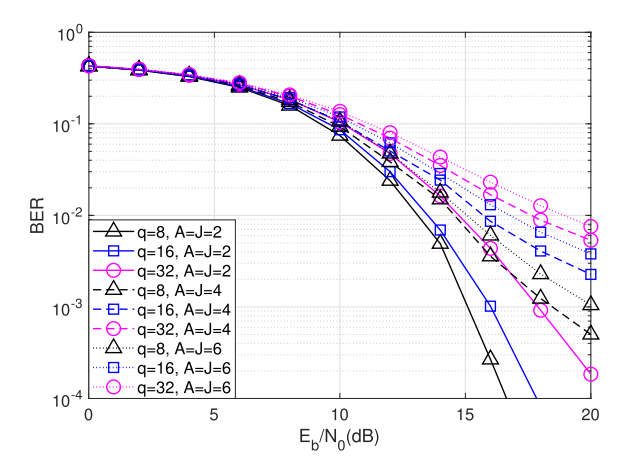


Fig. 8. Comparisons of the simulated BER of the SCS-MC-DCSK system with $\beta=128$, different q and different A over three-path Rayleigh fading channel.

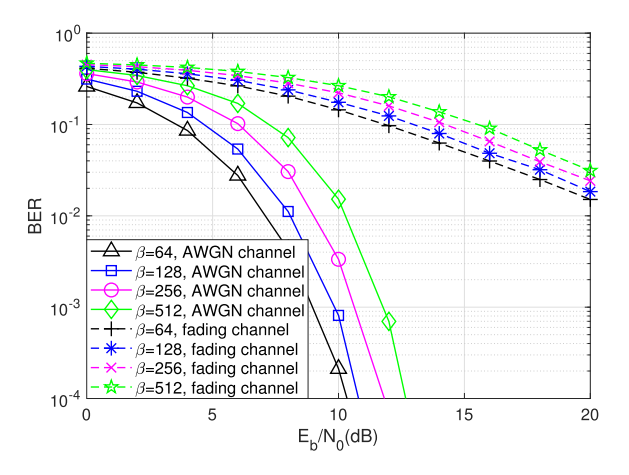


Fig. 9. Comparisons of the simulated BER of the SCS-MC-DCSK system with $A=6,\ J=6$ and different β over AWGN and fading channels.

the CC capacity. Different from the case of AWGN channel, Fig. 7(b) demonstrates that, the CC capacity of the system with A=1 is better than that with A=2 due to the larger distance between symbols.

C. BER Performance Comparisons

Next, we will investigate the simulated BER performances of the proposed system using different parameters, then we compare the BER performances with benchmark systems.

1) BER Performances With Different Parameters: Figure 8 and Fig. 9 respectively investigate the simulated BER performances with different settings. Fig. 8 illustrates the BER performances over the fading channel when q=8,16,32 and A=2,4,6. It can be observed that for smaller q=8 and A=J=2, better BER performances could be achieved thanks to larger distances between adjacent symbols and larger time diversity gain. Then Fig. 9 shows the simulated BER performances with different β over the AWGN channel and fading channel where $q=\beta$. Notably, $q=\beta$ means that the channel response will remain invariant during one symbol duration thus no time diversity gain can be utilized. It could

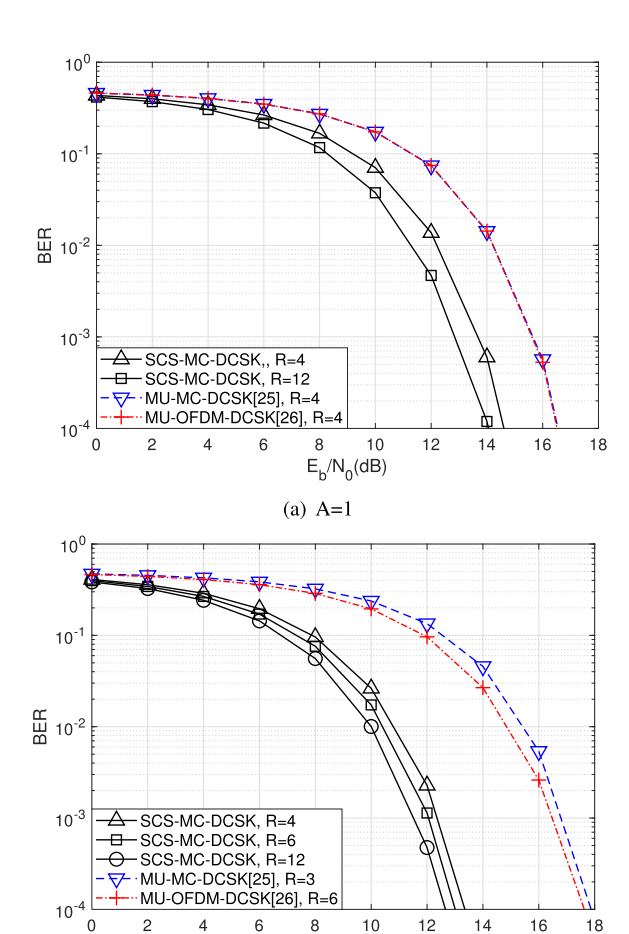


Fig. 10. Comparisons of the simulated BER of the SCS-MC-DCSK system and MU-MC-DCSK [25], MU-OFDM-DCSK [26] systems with $\beta=128$ over the AWGN channel.

(b) A=2

 $E_b/N_0(dB)$

be observed that when β increases, more interferences would be induced by chaotic signals, thereby leading to worse BER performances.

2) BER Performance Comparisons With Benchmark MC-DCSK Systems: In Fig. 10 and Fig. 11, we respectively compare the BER performances of the SCS-MC-DCSK system with two counterpart multi-user multi-carrier chaosmodulated schemes, i.e. the MU-MC-DCSK [25] and the MU-OFDM-DCSK [26] over the AWGN channel and the three-path Rayleigh fading channel.

Let R denote the number of transmitted bits in a symbol period, then for the proposed SCS-MC-DCSK system, $R = J \log_2 M$, while for the for MU-MC-DCSK, $R = K_{all} - A$, and for the MU-OFDM-DCSK system, $R = (K_{all} - A)A$. Note that for fairness of comparisons, we assume that all the systems have the same spectrum resources, i.e., $K_{all} = 5$.

Figure 10 illustrates the BER performances over AWGN channel. It can be seen that the proposed SCS-MC-DCSK system could achieve better BER performances than the other two benchmarks. Fig. 11 demonstrates that the proposed systems can also achieve better BER performances compared with benchmarks over the three-path Rayleigh fading channel with different q and different R. The reason is that our scheme

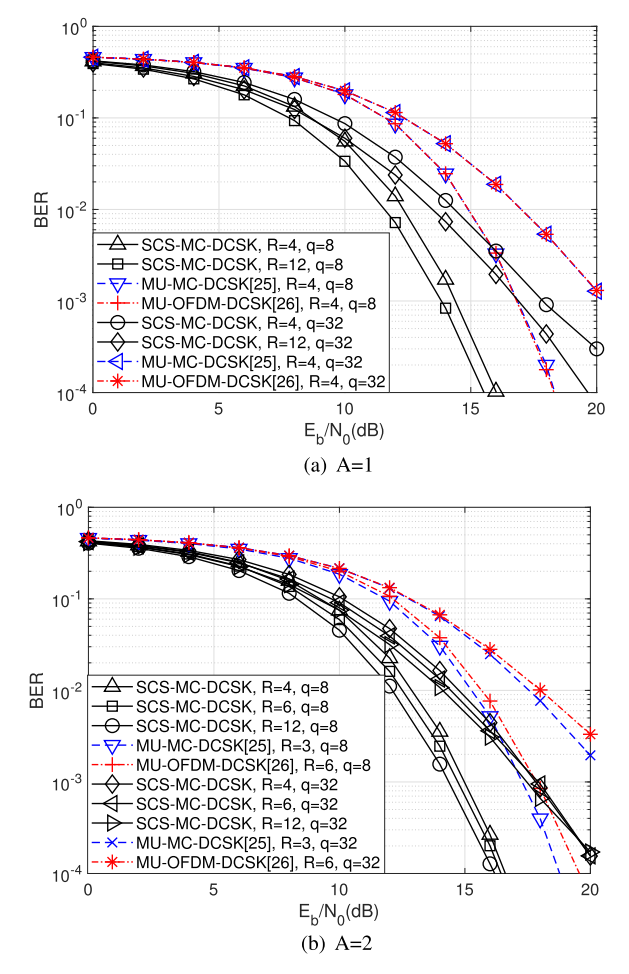


Fig. 11. Comparisons of the simulated BER of the SCS-MC-DCSK system and MU-MC-DCSK [25], MU-OFDM-DCSK [26] systems with $\beta=128$ over the three-path Rayleigh fading channel.

could benefit from the shaping gain brought by the multidimension constellation design, and attain higher efficiency since all UEs share the same reference signals. Besides, the MU-OFDM-DCSK scheme [26] suffers from much more serious MUIs than our scheme induced by the overlapping of signals from multiple UEs, thereby leading to worse reliability performances. In addition, we can also notice that when qis smaller, the time diversity gain will also increase, hence the BER performances with q=8 are better than those with q=32.

In addition, it is worth pointing out that the comparison given in Fig. 10(a) and Fig. 11(a) is fair since all schemes have the same data rate R=4 and the same spectrum resources. However, when A=2, although all considered schemes use the same number of subcarriers, they would have different data rate. Explicitly, the MU-MC-DCSK scheme has the data rate of R=3 as in [25], while the proposed system has the data rate of R=4 in both Fig. 10(b) and Fig. 11(b).

Moreover, it could be observed from Fig. 10 and Fig. 11 that for both AWGN and Rayleigh fading channels, the BER performances of the proposed system become better when R increases with the proportion $\frac{J+1}{J}$ decreases. The reason is that when $\frac{J+1}{J}$ decreases, N_0 will become smaller, thus the value of E_b/N_0 will increase, thereby leading to the improved

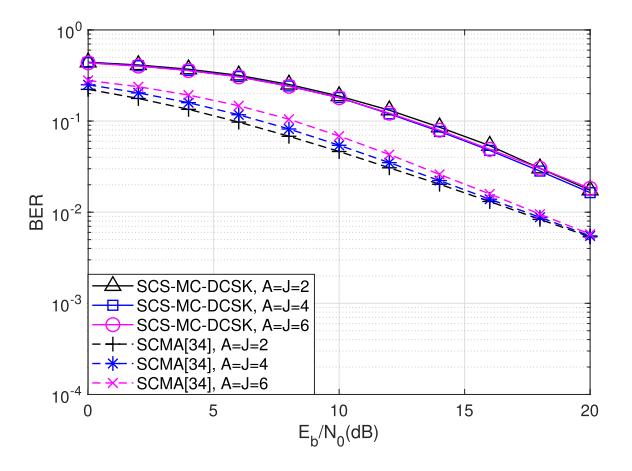


Fig. 12. Comparisons of BER performances of the SCS-MC-DCSK system and SCMA [34] over the three-path Rayleigh fading channel.

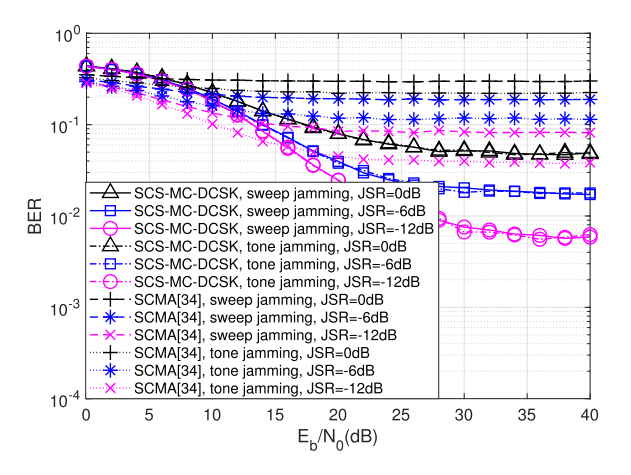


Fig. 13. BER performances of the SCS-MC-DCSK system and SCMA [34] over the three-path Rayleigh fading channel against jamming with A=J=6.

BER performances. To be more explicit, the bit energy is expressed as $E_b = \frac{(J+1)P}{J\log_2 M}$, while the noise power is denoted by $N_0 = \frac{J+1}{J} \frac{P}{\frac{E_b}{N_0}\log_2 M}$. Hence N_0 will decrease with smaller $\frac{J+1}{J}$, then a larger E_b/N_0 helps to enhance the reliability performances.

3) BER Performance Comparisons With SCMA: In Fig. 12 and Fig. 13, we compare the BER performances between the proposed scheme and the SCMA system [34], which also uses the MD receiver, over the three-path Rayleigh fading channel. Let T_o and $T_{o,SCMA}$ respectively represent the symbol duration of our scheme and the SCMA system. For fairness of comparisons, we have $T_{o,SCMA} = \beta T_o$ and $\beta = 128$ for SCS-MC-DCSK. Additionally, the channel coefficients maintain constant in the whole symbol duration, i.e. $q = \beta$.

In addition, in Fig. 13, we use the discrete baseband model of the sweep jamming signals and tone jamming signals given in [2], wherein the i_{th} jamming chip of the sweep jamming model is denoted as $\sqrt{2P_{jam}}\sin\left(2\pi iF_{start}/N_{jam}+\pi i^2\Delta F/N_{jam}^2\right)$ and the tone jamming model is denoted as $\sum_{m_{jam}}^{M_{jam}}\sqrt{2~P_{jam}/M_{jam}}\sin\left(2\pi iF_{m_{jam}}\right)$ where P_{jam} denotes the power of the jamming signal. Additionally, the

range of i is $0 \le i \le N_{jam} - 1$, F_{start} is set as 1, ΔF is set as 1, $M_{jam} = 3$ is the number of tones, $F_{m_{jam}}$ is set as [1,3,5]. Moreover, we assume that the cycle of the jamming signal is βT_o and thus, $N_{jam} = K_{all}\beta$, and the ratio of the jamming signal power to the signal power is defined as Jamming Signal Ratio (JSR).

It could be observed that the BER performances of the proposed SCS-MC-DCSK system are worse than those of the SCMA system when no jamming is existent. However, when wireless transmissions undergo the jamming such as the sweep jamming and the tone jamming, the proposed system achieves better BER performances. Hence the proposed design inherits the anti-jamming capability of chaotic transmissions and outperforms the SCMA system.

V. CONCLUSION

In this paper, we propose a SCS-MC-DCSK scheme to provide reliable services and high data rate by exploiting the non orthogonal spreading and the multi-dimension constellation shaping gain. In our design, we construct the sparse codes to spread the user data in the frequency domain and then modulate the information bits with the multi-dimension codebook, thus the Euclidean distance of adjacent symbols could be enlarged, while the data from multiple different users are allowed to overlap on the same sub-carriers. As a result, multiple users could share all frequency band resources for information transmissions. Besides, all the users will share the same reference chaotic signal carried by one subcarrier in different layers, thus the diversity gain could be exploited to improve the quality of the reference signal. At the receiver, we propose a MD detector to identify the data from different users and to retrieve the estimates. Moreover, we derive the theoretical UB of the SER expressions and CC capacity over the AWGN and the multipath Rayleigh fading channel, and compare the spectrum efficiency, energy efficiency as well as the complexity with benchmark schemes. Simulation results verify the effectiveness of theoretical derivations, and demonstrate that our proposed system achieves better BER performances than MU-MC-DCSK and MU-OFDM-DCSK systems, while providing higher capacity as well as has better anti-jamming capability than SCMA systems. Therefore, with the aid of the sparse coding and the multi-dimension codebook, better reliability and higher data rate could be achieved by the proposed multiuser MC-DCSK systems. Last but not the least, it is worth mentioning that the proposed scheme could be applied in systems with massive connections such as the machine type communications to provide efficient and reliable services for multiple users.

REFERENCES

- [1] F. C. M. Lau, M. Ye, C. K. Tse, and S. F. Hau, "Anti-jamming performance of chaotic digital communication systems," *IEEE Trans. Circuits Syst. I, Fundam. Theory Appl.*, vol. 49, no. 10, pp. 1486–1494, Oct. 2002.
- [2] B. Van Nguyen, H. Jung, and K. Kim, "On the antijamming performance of the NR-DCSK system," *Hindawi Secur. Commun. Netw.*, vol. 2018, Feb. 2018, Art. no. 7963641.
- [3] F. C. M. Lau and C. K. Tse, Chaos-Based Digital Communication Systems: Operating Principles, Analysis Methods, and Performance Evaluation. Berlin, Germany: Springer, 2003.

- [4] G. Kolumbán, B. Vizvári, W. Schwarz, and A. Abel, "Differential chaos shift keying: A robust coding for chaos communication," in *Proc. Int.* Workshop Nonlinear Dyn. Electron. Syst. (NDES), Jun. 1996, pp. 87–92.
- [5] P. Chen, Y. Fang, G. Han, and G. Chen, "An efficient transmission scheme for DCSK cooperative communication over multipath fading channels," *IEEE Access*, vol. 4, pp. 6364–6373, Sep. 2016.
- [6] G. Cai, Y. Fang, G. Han, J. Xu, and G. Chen, "Design and analysis of relay-selection strategies for two-way relay network-coded DCSK systems," *IEEE Trans. Veh. Technol.*, vol. 67, no. 2, pp. 1258–1271, Feb. 2018.
- [7] F. J. Escribano, G. Kaddoum, A. Wagemakers, and P. Giard, "Design of a new differential chaos-shift-keying system for continuous mobility," *IEEE Trans. Commun.*, vol. 64, no. 5, pp. 2066–2078, May 2016.
- [8] H. Ma, G. Cai, Y. Fang, J. Wen, P. Chen, and S. Akhtar, "A new enhanced energy-detector-based FM-DCSK UWB system for tactile Internet," *IEEE Trans. Ind. Informat.*, vol. 15, no. 5, pp. 3028–3039, May 2019.
- [9] G. Cai, Y. Fang, P. Chen, G. Han, G. Cai, and Y. Song, "Design of an MISO-SWIPT-aided code-index modulated multi-carrier M-DCSK system for e-health IoT," *IEEE J. Sel. Areas Commun.*, early access, Sep. 01, 2020, doi: 10.1109/jsac.2020.3020603.
- [10] Z. Galias and G. M. Maggio, "Quadrature chaos-shift keying: Theory and performance analysis," *IEEE Trans. Circuits Syst. I, Fundam. Theory Appl.*, vol. 48, no. 12, pp. 1510–1519, Dec. 2001.
- [11] A. Kumar and P. R. Sahu, "Performance analysis of spatially modulated differential chaos shift keying modulation," *IET Commun.*, vol. 11, no. 6, pp. 905–909, Apr. 2017.
- [12] M. Miao, L. Wang, M. Katz, and W. Xu, "Hybrid modulation scheme combining PPM with differential chaos shift keying modulation," *IEEE Wireless Commun. Lett.*, vol. 8, no. 2, pp. 340–343, Apr. 2019.
- [13] H. Ma, G. Cai, Y. Fang, P. Chen, and G. Chen, "Design of a superposition coding PPM-DCSK system for downlink multi-user transmission," IEEE Trans. Veh. Technol., vol. 69, no. 2, pp. 1666–1678, Feb. 2020.
- [14] W. K. Xu, L. Wang, and G. Kolumbán, "A novel differential chaos shift keying modulation scheme," *Int. J. Bifurcation Chaos*, vol. 21, no. 3, pp. 799–814, Mar. 2011.
- [15] T. Huang, W. Xu, L. Wang, and F. C. M. Lau, "Multilevel code-shifted differential-chaos-shift-keying system," *IET Commun.*, vol. 10, no. 10, pp. 1189–1195, Jul. 2016.
- [16] X. Cai, W. Xu, R. Zhang, and L. Wang, "A multilevel code shifted differential chaos shift keying system with M-ary modulation," *IEEE Trans. Circuits Syst. II, Exp. Briefs*, vol. 66, no. 8, pp. 1451–1455, Aug. 2019.
- [17] Y. Tan, W. Xu, T. Huang, and L. Wang, "A multilevel code shifted differential chaos shift keying scheme with code index modulation," *IEEE Trans. Circuits Syst. II, Exp. Briefs*, vol. 65, no. 11, pp. 1743–1747, Nov. 2018.
- [18] G. Kolumban, G. Kis, Z. Jako, and M. P. Kennedy, "FM-DCSK: A robust modulation scheme for chaotic communications," *IEICE Trans. Fundam. Electron., Commun. Comput. Sci.*, vols. E81–A, no. 9, pp. 1798–1802, Oct. 1998.
- [19] G. Kaddoum, F.-D. Richardson, and F. Gagnon, "Design and analysis of a multi-carrier differential chaos shift keying communication system," *IEEE Trans. Commun.*, vol. 61, no. 8, pp. 3281–3291, Aug. 2013.
- [20] G. Cheng, L. Wang, W. Xu, and G. Chen, "Carrier index differential chaos shift keying modulation," *IEEE Trans. Circuits Syst. II, Exp. Briefs*, vol. 64, no. 8, pp. 907–911, Aug. 2017.
- [21] G. Cheng, X. Chen, W. Liu, and W. Xiao, "GCI-DCSK: Generalized carrier index differential chaos shift keying modulation," *IEEE Commun. Lett.*, vol. 23, no. 11, pp. 2012–2016, Nov. 2019.
- [22] G. Cai, Y. Fang, J. Wen, S. Mumtaz, Y. Song, and V. Frascolla, "Multi-carrier M-ary DCSK system with code index modulation: An efficient solution for chaotic communications," *IEEE J. Sel. Topics Signal Process.*, vol. 13, no. 6, pp. 1375–1386, Oct. 2019.
- [23] X. Cai, W. Xu, L. Wang, and G. Kolumban, "Multicarrier M-ary orthogonal chaotic vector shift keying with index modulation for high data rate transmission," *IEEE Trans. Commun.*, vol. 68, no. 2, pp. 974–986, Feb. 2020.
- [24] Z. Liu, L. Zhang, and Z. Chen, "Low PAPR OFDM-based DCSK design with carrier interferometry spreading codes," *IEEE Commun. Lett.*, vol. 22, no. 8, pp. 1588–1591, Aug. 2018.
- [25] G. Kaddoum, F.-D. Richardson, S. Adouni, F. Gagnon, and C. Thibeault, "Multi-user multi-carrier differential chaos shift keying communication system," in *Proc. 9th Int. Wireless Commun. Mobile Comput. Conf.* (IWCMC), Jul. 2013, pp. 1798–1802.

- [26] G. Kaddoum, "Design and performance analysis of a multiuser OFDM based differential chaos shift keying communication system," *IEEE Trans. Commun.*, vol. 64, no. 1, pp. 249–260, Jan. 2016.
- [27] G. Kaddoum and F. Shokraneh, "Analog network coding for multiuser multi-carrier differential chaos shift keying communication system," *IEEE Trans. Wireless Commun.*, vol. 14, no. 3, pp. 1492–1505, Mar. 2015.
- [28] B. Chen, L. Zhang, and Z. Wu, "General iterative receiver design for enhanced reliability in multi-carrier differential chaos shift keying systems," *IEEE Trans. Commun.*, vol. 67, no. 11, pp. 7824–7839, Nov. 2019.
- [29] Z. Liu, L. Zhang, Z. Wu, and J. Bian, "A secure and robust frequency and time diversity aided OFDM–DCSK modulation system not requiring channel state information," *IEEE Trans. Commun.*, vol. 68, no. 3, pp. 1684–1697, Mar. 2020.
- [30] H. Nikopour and H. Baligh, "Sparse code multiple access," in *Proc. IEEE Int. Symp. Pers. Indoor Mobile Radio Commun.*, London, U.K., Sep. 2013, pp. 332–336.
- [31] M. Taherzadeh, H. Nikopour, A. Bayesteh, and H. Baligh, "SCMA codebook design," in *Proc. IEEE 80th Veh. Technol. Conf. (VTC-Fall)*, Sep. 2014, pp. 1–5.
- [32] Z. Wu, K. Lu, C. Jiang, and X. Shao, "Comprehensive study and comparison on 5G NOMA schemes," *IEEE Access*, vol. 6, pp. 18511–18519, Mar. 2018.
- [33] M. Vameghestahbanati, I. D. Marsland, R. H. Gohary, and H. Yanikomeroglu, "Multidimensional constellations for uplink SCMA systems—A comparative study," *IEEE Commun. Surveys Tuts.*, vol. 21, no. 3, pp. 2169–2194, 3rd Quart., 2019.
- [34] S. M. Hasan, K. Mahata, and M. M. Hyder, "Sparse code multiple access codebook design using equiangular tight frames," in *Proc. IEEE Int. Conf. Commun. (ICC)*, Jun. 2020, pp. 1–6.
- [35] D. Tse and P. Viswanath, *Fundamentals of Wireless Communication*. Cambridge, U.K.: Cambridge Univ. Press, Sep. 2004.
- [36] L. Zhang, Z. Chen, W. Rao, and Z. Wu, "Efficient and secure non-coherent OFDM-based overlapped chaotic chip position shift keying system: Design and performance analysis," *IEEE Trans. Circuits Syst. I, Reg. Papers*, vol. 67, no. 1, pp. 309–321, Jan. 2020.
- [37] Y. Xia, C. K. Tse, and F. C. M. Lau, "Performance of differential chaos-shift-keying digital communication systems over a multipath fading channel with delay spread," *IEEE Trans. Circuits Syst. II, Exp. Briefs*, vol. 51, no. 12, pp. 680–684, Dec. 2004.
- [38] J. Wu, J. Li, D. Xie, and F. Fan, "The Monte Carlo calculation method of multiple integration," in *Proc. 11th Int. Comput. Conf. Wavelet Actiev Media Technol. Inf. Process. (ICCWAMTIP)*, Dec. 2014, pp. 491–494.
- [39] J. Bao, Z. Ma, G. K. Karagiannidis, M. Xiao, and Z. Zhu, "Joint multiuser detection of multidimensional constellations over fading channels," *IEEE Trans. Commun.*, vol. 65, no. 1, pp. 161–172, Jan. 2017.



Zuwei Chen received the B.S. degree from the School of Electronic Information Science and Technology, Sun Yat-sen University, Guangzhou, China, in 2019. He is currently pursuing the master's degree with the School of Information and Communication Engineering, Sun Yat-sen University. His research interests include chaotic communication and its application to wireless communication systems.



Lin Zhang (Senior Member, IEEE) received the Ph.D. degree in information and communication engineering from Sun Yat-sen University in 2003. In 2003, she joined the School of Information Science and Technology, Sun Yat-sen University, where she has been an Associate Professor since 2007. From 2008 to 2009, she was a Visiting Researcher with the Electrical and Computer Engineering Department, University of Maryland, College Park, USA. In 2016, she joined the School of Electronics and Information Technology, Sun Yat-

sen University. She is also with the Southern Marine Science and Engineering Guangdong Laboratory. Her research has been supported by the National Natural Science Foundation of China and the Science and Technology Program Project of Guangdong Province. Her current research interests are in the area of signal processing and their applications to wireless communication systems.



Zhiqiang Wu (Senior Member, IEEE) received the B.S. degree from the Beijing University of Posts and Telecommunications in 1993, the M.S. degree from Peking University in 1996, and the Ph.D. degree from Colorado State University in 2002, all in electrical engineering. He was an Assistant Professor with the Department of Electrical and Computer Engineering, Institute of Technology, West Virginia University, from 2003 to 2005. In 2005, he joined Wright State University, where he is currently a Full Professor with the Department of Electrical

Engineering. He has also held visiting positions at Peking University, Harbin Engineering University, Guizhou Normal University, and Tibet University. His research has been supported by NSF, AFRL, ONR, AFOSR, and OFRN.



Lin Wang (Senior Member, IEEE) received the M.Sc. degree in applied mathematics from the Kunming University of Technology, China, in 1988, and the Ph.D. degree in electronics engineering from the University of Electronic Science and Technology of China, China, in 2001. From 1984 to 1986, he was a Teaching Assistant with the Mathematics Department, Chongqing Normal University. From 1989 to 2002, he was a Teaching Assistant, a Lecturer, and then an Associate Professor in applied mathematics and communication engineering with the Chongqing

University of Posts and Telecommunications, China. From 1995 to 1996, he was with the Mathematics Department, University of New England, Armidale, NSW, Australia. In 2003, he was a Visiting Researcher with the Center for Chaos and Complexity Networks, Department of Electronic Engineering, City University of Hong Kong, for three months. In 2013, he was a Senior Visiting Researcher with the Department of Electrical and Computer Engineering, University of California at Davis, Davis, CA, USA. From 2003 to 2012, he was a Full Professor and an Associate Dean with the School of Information Science and Engineering, Xiamen University, China. He has been a Distinguished Professor since 2012. He holds 14 patents in the field of physical layer in digital communications. He has authored over 100 journal and conference papers. His current research interests are in the areas of channel coding, joint source and channel coding, chaos modulation, and their applications to wireless communication and storage systems.



Weikai Xu (Member, IEEE) received the B.S. degree in electronic engineering from the Three Gorges College, Chongqing, China, in 2000, the M.Sc. degree in communication and information system from the Chongqing University of Posts and Telecommunications, Chongqing, China, in 2003, and the Ph.D. degree in electronic circuit and system from the Xiamen University of China, Xiamen, China, in 2011. From 2003 to 2012, he was a Teaching Assistant and an Assistant Professor in communication engineering with Xiamen University.

He is currently an Associate Professor in information and communication engineering with Xiamen University. His research interests include chaotic communications, underwater acoustic communications, channel coding, cooperative communications, and ultra-wideband.